UNIVERSITY OF BRISTOL

University of Bristol - Explore Bristol Research
General rights

Measurement of the J/ψ pair production cross-section in pp collisions at $\sqrt{s} = 13$ TeV

The LHCb collaboration

E-mail: liupan.an@cern.ch

ABSTRACT: The production cross-section of J/ψ pairs is measured using a data sample of pp collisions collected by the LHCb experiment at a centre-of-mass energy of $\sqrt{s} = 13$ TeV, corresponding to an integrated luminosity of $279 \pm 11\,\text{pb}^{-1}$. The measurement is performed for J/ψ mesons with a transverse momentum of less than $10\,\text{GeV}/c$ in the rapidity range $2.0 < y < 4.5$. The production cross-section is measured to be $15.2 \pm 1.0 \pm 0.9\,\text{nb}$. The first uncertainty is statistical, and the second is systematic. The differential cross-sections as functions of several kinematic variables of the J/ψ pair are measured and compared to theoretical predictions.

Contents

1 Introduction

The production mechanism of heavy quarkonia is a long-standing and intriguing problem in quantum chromodynamics (QCD), which is not fully understood even after over forty years of study. The colour-singlet model (CSM) [1–10] assumes the intermediate $Q\overline{Q}$ state to be colourless and to have the same J^{PC} quantum numbers as the final quarkonium state. Leading-order calculations in the CSM underestimate the J/ψ and $\psi(2S)$ production cross-sections at high transverse momentum, p_{T}, by more than one order of magnitude [11]. The gap between CSM predictions and experimental measurements is reduced when including next-to-leading-order corrections, but the agreement is still not satisfactory [12–14]. The non-relativistic QCD (NRQCD) model takes into account both colour-singlet (CS) and colour-octet (CO) states of the $Q\overline{Q}$ pair [15–17]. It either describes the production cross-sections and polarisations at large p_{T} or it describes the production cross-section at all p_{T} values, but then fails to predict the polarisation [18–33]. This puzzle can be probed via the production of pairs of quarkonia [34–39], where the interpretation of the measured cross-section could be simpler. In quarkonium-pair production, the selection rules in the CS process of leading-order (LO) NRQCD forbid the feed-down from cascade decays of excited C-even states. This feed-down from C-even states, e.g. $\chi_c \to J/\psi\,\gamma$ or $\chi_b \to \Upsilon\gamma$, plays an important role in single quarkonium production. It significantly complicates the precise comparison between data and model predictions, and makes the interpretation of polarisation measurements difficult.

    Besides the single parton scattering (SPS) process, the process of double parton scattering (DPS) can also contribute to quarkonium pair production. The DPS process is of great

importance since it can provide information on the transverse momenta of the partons and their correlations inside the proton, and can help in understanding various backgrounds, e.g. $Z + b\bar{b}$, $W^+ + W^-$, multi-jets etc., in searches for new physics. The DPS processes have been studied in several final states, e.g. 4-jets by the AFS [40], UA2 [41], CDF [42], and ATLAS [43] collaborations, $\gamma + 3$-jets by the CDF [44] and D0 [45, 46] collaborations, $2\gamma + 2$-jets by the D0 [47] collaboration, $W + 2$-jets [48] and $\Upsilon + \Upsilon$ [49] by the CMS collaboration, $J/\psi + W$ [50] and $J/\psi + Z$ [51] by the ATLAS collaboration, and double charm [52], Z + open charm [53] and Υ + open charm [54] by the LHCb collaboration. After having been first observed by the NA3 collaboration in pion-nuclear and proton-nuclear interactions [55, 56], J/ψ pair production has been measured in pp collisions by the LHCb [57] and CMS [58] experiments at $\sqrt{s} = 7\,\mathrm{TeV}$ and by the ATLAS experiment [59] at $\sqrt{s} = 8\,\mathrm{TeV}$. The D0 experiment [60] measured it using $p\bar{p}$ collision data at $\sqrt{s} = 1.96\,\mathrm{TeV}$.

Within the DPS mechanism, two quarkonia are produced independently in different partonic interactions. Neglecting the parton correlations in the proton, the contribution of this mechanism is estimated according to the formula [61–63]

$$\sigma_{\mathrm{DPS}}\left(J/\psi\,J/\psi\right) = \frac{1}{2}\frac{\sigma\left(J/\psi\right)^2}{\sigma_{\mathrm{eff}}}, \tag{1.1}$$

where $\sigma(J/\psi)$ is the inclusive prompt J/ψ production cross-section, the factor $1/2$ accounts for two identical particles in the final state, and σ_{eff} is an effective cross-section, which provides a proper normalisation of the DPS cross-section estimate. The effective cross-section is related to the transverse overlap function between partons in the proton, and is thought to be universal for all processes and energy scales. Most of the measured values of σ_{eff} lie in the range $12 - 20\,\mathrm{mb}$ [43, 54, 64], which supports the expectation that σ_{eff} is universal for a large range of processes with different kinematics and scales, and for a wide spectrum of centre-of-mass energies in pp and $p\bar{p}$ collisions.

The LHCb measurement of $\sigma\left(J/\psi\,J/\psi\right) = 5.1 \pm 1.0 \pm 1.1\,\mathrm{nb}$ at $\sqrt{s} = 7\,\mathrm{TeV}$ is not precise enough to distinguish between the SPS and DPS contributions [65, 66]. The SPS contribution is calculated to be $4.0 \pm 1.2\,\mathrm{nb}$ [67, 68] and $4.6 \pm 1.1\,\mathrm{nb}$ [39] in the leading-order NRQCD CS approach, and $5.4^{+2.7}_{-1.1}\,\mathrm{nb}$ [39] using complete next-to-leading order NRQCD CS approach. The DPS contribution is estimated to be $3.8 \pm 1.3\,\mathrm{nb}$ with eq. (1.1) using $\sigma\left(J/\psi\right)$ from ref. [69] and $\sigma_{\mathrm{eff}} = 14.5 \pm 1.7^{+1.7}_{-2.3}\,\mathrm{mb}$ from ref. [44]. The large number of reconstructed J/ψ pair events in the CMS data [58] allowed for study of J/ψ correlations [70]. The observation of events with a large separation in rapidity of two J/ψ mesons indicates a significant DPS contribution, leading to $\sigma_{\mathrm{eff}} = 8.2 \pm 2.2\,\mathrm{mb}$ [70], somewhat lower than the majority of other σ_{eff} measurements. A similarly small value, $\sigma_{\mathrm{eff}} = 6.3 \pm 1.9\,\mathrm{mb}$, is obtained by the ATLAS collaboration using a data-driven model-independent approach [59]. A small value of $\sigma_{\mathrm{eff}} = 4.8 \pm 2.5\,\mathrm{mb}$ is also obtained by the D0 collaboration [60] using the separation of the two J/ψ mesons in pseudorapidity to distinguish SPS and DPS contributions. Together with an even smaller value of $\sigma_{\mathrm{eff}} = 2.2 \pm 1.1\,\mathrm{mb}$, determined by the D0 collaboration from the measurement of the simultaneous production of J/ψ and Υ mesons [71], and the estimate of $\sigma_{\mathrm{eff}} = 2.2 - 6.6\,\mathrm{mb}$ by

the CMS collaboration from the production of Υ pairs [49], these results question the universality of σ_{eff}.

In this paper, the J/ψ pair production cross-section is measured using pp collision data collected by the LHCb experiment in 2015 at $\sqrt{s} = 13\,\text{TeV}$ with both J/ψ mesons in the rapidity range $2.0 < y < 4.5$, and with a transverse momentum $p_{\text{T}} < 10\,\text{GeV}/c$. The polarisation of the J/ψ mesons is assumed to be zero since there is as yet no knowledge of the polarisation of J/ψ pairs, and all the LHC analyses indicate a small polarisation for the quarkonia [29–33]. The J/ψ mesons are reconstructed via the $\mu^+\mu^-$ final state. In the following, the labels J/ψ_1 and J/ψ_2 are randomly assigned to the two J/ψ candidates.

2 Detector and data set

The LHCb detector [72, 73] is a single-arm forward spectrometer covering the pseudorapidity range $2 < \eta < 5$, designed for the study of particles containing b or c quarks. The detector includes a high-precision tracking system consisting of a silicon-strip vertex detector surrounding the pp interaction region, a large-area silicon-strip detector (TT) located upstream of a dipole magnet with a bending power of about $4\,\text{Tm}$, and three stations of silicon-strip detectors and straw drift tubes placed downstream of the magnet. The tracking system provides a measurement of momentum, p, of charged particles with a relative uncertainty that varies from 0.5% at low momentum to 1.0% at $200\,\text{GeV}/c$. The minimum distance of a track to a primary vertex (PV), the impact parameter, is measured with a resolution of $(15 + 29/p_{\text{T}})\,\mu\text{m}$, where p_{T} is in GeV/c. Different types of charged hadrons are distinguished using information from two ring-imaging Cherenkov detectors. Photons, electrons and hadrons are identified by a calorimeter system consisting of scintillating-pad and preshower detectors, an electromagnetic calorimeter and a hadronic calorimeter. Muons are identified by a system composed of alternating layers of iron and multiwire proportional chambers.

The online event selection is performed by a trigger [74], which consists of a hardware stage (L0), based on information from the calorimeter and muon systems, followed by a software stage, which applies a full event reconstruction. The L0 trigger requires two muons with $p_{\text{T}}(\mu_1) \times p_{\text{T}}(\mu_2) > (1.3\,\text{GeV}/c)^2$. In the first stage of the software trigger (HLT1), two muons with $p_{\text{T}} > 330\,\text{MeV}/c$ and $p > 6\,\text{GeV}/c$ are required to form a J/ψ candidate with invariant mass $M(\mu^+\mu^-) > 2.7\,\text{GeV}/c^2$; alternatively, the event can also be accepted when it has a good quality muon with $p_{\text{T}} > 4.34\,\text{GeV}/c$ and $p > 6\,\text{GeV}/c$. In the second stage of the software trigger (HLT2), the two J/ψ mesons are reconstructed from $\mu^+\mu^-$ pairs with good vertex-fit quality and invariant masses within $\pm 120\,\text{MeV}/c^2$ of the known J/ψ mass [75], using algorithms identical to the offline reconstruction. In the offline selection, all four muons in the final state are required to have $p_{\text{T}} > 650\,\text{MeV}/c$, $6 < p < 200\,\text{GeV}/c$ and $2 < \eta < 5$. Each track must have a good-quality track fit and be identified as a muon. The four muon tracks are required to originate from the same PV. This reduces to a negligible level the number of pile-up candidates, i.e. J/ψ pairs from two independent pp interactions. The reconstructed J/ψ mesons are required to have a good-quality vertex and an invariant mass in the range $3000 < M(\mu^+\mu^-) < 3200\,\text{MeV}/c^2$. Only events explicitly

triggered by one of the J/ψ candidates at the L0 and the HLT1 stages are retained. For events with multiple candidates, in particular where the four muons can be combined in two different ways to form a J/ψ pair, which account for 1.4% of the total candidates, one randomly chosen candidate pair is retained.

Simulated J/ψ samples are generated to study the behaviour of the signal. In the simulation, pp collisions are generated using PYTHIA8 [76, 77] with a specific LHCb configuration [78]. Decays of hadronic particles are described by EVTGEN [79], in which final-state radiation is generated using PHOTOS [80]. The interaction of the generated particles with the detector, and its response, are implemented using the GEANT4 toolkit [81] as described in ref. [82].

3 Cross-section determination

The inclusive J/ψ pair production cross-section is measured as

$$\sigma(J/\psi\, J/\psi) = \frac{N^{\text{cor}}}{\mathcal{L} \times \mathcal{B}(J/\psi \to \mu^+\mu^-)^2}, \tag{3.1}$$

where N^{cor} is the number of signal candidates after the efficiency correction, $\mathcal{B}(J/\psi \to \mu^+\mu^-) = (5.961 \pm 0.033)\%$ is the branching fraction of the $J/\psi \to \mu^+\mu^-$ decay [75], and $\mathcal{L} = 279 \pm 11\,\text{pb}^{-1}$ is the integrated luminosity, determined using the beam-gas imaging and van der Meer scan methods [83].

The total detection efficiency of the J/ψ pair is estimated as

$$\varepsilon_{\text{tot}} = \varepsilon_{\text{acc}} \times \varepsilon_{\text{rec\&sel}} \times \varepsilon_{\text{PID}} \times \varepsilon_{\text{trig}}, \tag{3.2}$$

where ε_{acc} is the geometrical acceptance, $\varepsilon_{\text{rec\&sel}}$ is the reconstruction and selection efficiency for candidates with all final-state muons inside the geometrical acceptance, ε_{PID} is the muon particle identification (PID) efficiency for selected candidates, and $\varepsilon_{\text{trig}}$ is the trigger efficiency for selected candidates satisfying the PID requirement. The first three efficiencies of the J/ψ pair, ε_{acc}, $\varepsilon_{\text{rec\&sel}}$ and ε_{PID}, are factorized as

$$\varepsilon\left(J/\psi\, J/\psi\right) = \varepsilon\left(J/\psi_1\right) \times \varepsilon\left(J/\psi_2\right). \tag{3.3}$$

Since the HLT2 trigger selection is performed using the same reconstruction algorithm as the offline selection and the selection criteria of the HLT2 trigger are a subset of those used in the final selection, the corresponding trigger efficiency for the reconstructed and selected events is 100%. Since at least one of the two J/ψ meson candidates is required to have passed the L0 and HLT1 trigger, the efficiency $\varepsilon_{\text{trig}}$ of the J/ψ pair can be expressed as

$$\varepsilon_{\text{trig}}\left(J/\psi\, J/\psi\right) = 1 - \left(1 - \varepsilon_{\text{trig}}\left(J/\psi_1\right)\right) \times \left(1 - \varepsilon_{\text{trig}}\left(J/\psi_2\right)\right). \tag{3.4}$$

All terms in the single J/ψ efficiency are estimated in bins of p_{T} and y of the J/ψ mesons using the simulation. The track reconstruction and muon PID efficiency are corrected using data-driven techniques, as described in section 4, and the trigger efficiency measurement is validated on data.
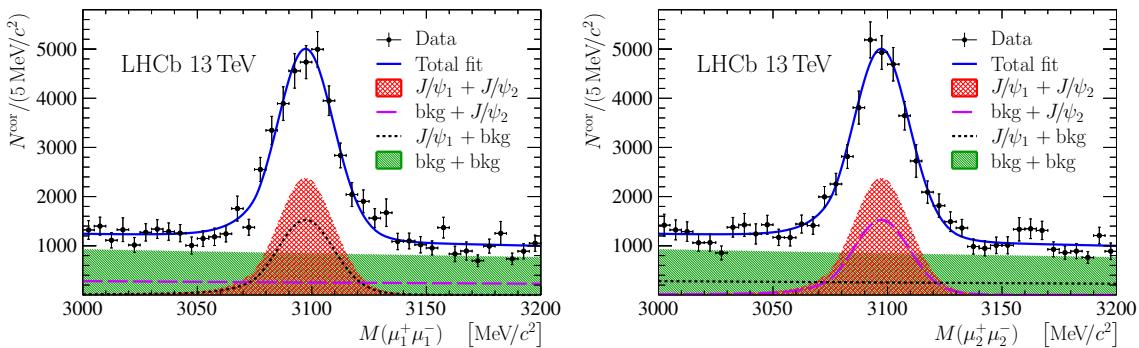
Figure 1. Projections of the fit to the efficiency-corrected distribution of the reconstructed J/ψ mass for (left) $M(\mu_1^+\mu_1^-)$ and (right) $M(\mu_2^+\mu_2^-)$. The (black) points with error bars represent the data. The (blue) solid line is the total fit function. The (red) cross-hatched area shows the signal distribution. The (black and magenta) dashed lines represent the background components due to the combination of a real J/ψ with a combinatorial candidate. The (green) shaded area shows the purely combinatorial background.

The signal yield is determined by performing an extended unbinned maximum likelihood fit to the efficiency-corrected two-dimensional $(M(\mu_1^+\mu_1^-), M(\mu_2^+\mu_2^-))$ mass distribution. The total detection efficiency is applied individually on an event-by-event basis. The signal is modelled by the sum of a double-sided Crystal Ball (DSCB) function [84] and a Gaussian function, which share the same mean value. The power law tail parameters of the DSCB, the relative fraction and the difference between the widths of the DSCB and the Gaussian function are fixed to the values obtained from simulation, leaving the peak value and the core width of the DSCB as free parameters. The combinatorial background is described by an exponential function. Since the labels J/ψ_1 and J/ψ_2 are assigned randomly, the fit function is symmetric under the exchange of the J/ψ_1 and J/ψ_2 masses. The fit projections on $M(\mu_1^+\mu_1^-)$ and $M(\mu_2^+\mu_2^-)$ are shown in figure 1. The corrected yield[1] of J/ψ pairs is determined to be $N^{\text{cor}} = (15.8 \pm 1.1) \times 10^3$.

After the fit, the residual contamination, where either one or both J/ψ mesons come from b-hadron decays, must be corrected for. The fraction of background is evaluated with the help of simulation validated with data and normalized using the measured prompt J/ψ and inclusive $b\bar{b} \to J/\psi$ production cross-sections within the LHCb acceptance at $\sqrt{s} = 13\,\text{TeV}$ [85]. The fraction of candidates with J/ψ mesons from b-hadron decays is determined to be 4.5%.

4   Systematic uncertainties

Several sources of systematic uncertainties on the J/ψ pair production cross-section are studied and summarized in table 1. The uncertainty due to the signal shape description is estimated by replacing the nominal model with two alternative models, the Hypatia function [86] and a kernel estimate for the underlying probability distribution function of

---

[1]The corresponding fit of the efficiency-uncorrected sample gives $(1.05 \pm 0.05) \times 10^3$ signal events.

the simulated sample convolved with a Gaussian function [87]. The relative difference of 1.6% with respect to the nominal result is taken as a systematic uncertainty.

A difference between simulation and data, in particular in the fit quality of the candidates when constraining the muons to the PV, can lead to a bias in the efficiency determination. This is estimated by comparing the vertex-fit quality of the reconstructed J/ψ candidates between the simulated and the data samples, where the background is subtracted using the *sPlot* technique [88]. Data and simulation agree within 1.0%, which is taken as a systematic uncertainty.

The track reconstruction efficiency is studied in data using a tag-and-probe technique [89]. In this method, one of the muons from the J/ψ is fully reconstructed as the tag track, and the other muon track, the probe track, is reconstructed using only information from the TT detector and the muon stations. The tracking efficiency is taken as the fraction of J/ψ candidates whose probe tracks match fully reconstructed tracks. The simulated sample is corrected to match the track multiplicity of events in the data. The ratio of tracking efficiencies between data and simulation is taken as the correction factor. A systematic uncertainty of 0.8% per track is assigned for the difference in event multiplicity between data and simulation.

The muon PID efficiency is also determined using a tag-and-probe method [90], where only one track of the J/ψ is identified as a muon, i.e. the tag track. The single muon PID efficiency, defined as the fraction of J/ψ candidates with the other track (probe track) identified as a muon, is determined in bins of p and η of the probe track. Systematic effects arising from the choice of the binning scheme and for the difference in event multiplicity between data and simulation are studied. In total, the muon PID efficiency uncertainty is determined to be 2.3%.

The trigger efficiency $\varepsilon_{\rm trig}(J/\psi)$ measured with simulation is compared with the result obtained in data for inclusive J/ψ events using a tag-and-probe method [74]. A difference of 1.0% between the two results is observed and is taken as the systematic uncertainty.

An uncertainty of 1.0% is assigned to the determination of the fraction of candidates from b-hadron decays, which accounts for the uncertainty of the prompt J/ψ and $b\bar{b}$ production cross-sections. The uncertainty introduced by the limited statistics of the simulated samples used to determine the efficiencies is estimated to be negligible. The 1.1% uncertainty on $\mathcal{B}(J/\psi \to \mu^+\mu^-)$ is propagated to the cross-section. The systematic uncertainty due to the luminosity calibration is 3.9%. The total systematic uncertainty is 6.1%.

5   Results and comparison to theory

The J/ψ pair production cross-section where both J/ψ mesons are in the region $2.0 < y < 4.5$ and $p_{\rm T} < 10\,{\rm GeV}/c$ is measured to be

$$\sigma(J/\psi\,J/\psi) = 15.2 \pm 1.0\,({\rm stat}) \pm 0.9\,({\rm syst})\,{\rm nb},$$

assuming negligible polarisation of the J/ψ mesons. The detection efficiency of J/ψ mesons can be affected by the polarisation, especially by the polarisation parameter λ_θ in the helicity frame [32, 85]. If a value of $\lambda_\theta = \pm 20\%$ is assumed for both of the J/ψ mesons,

Source	Uncertainty[%]
Signal shape	1.6
Data/simulation difference	1.0
Tracking efficiency	0.8×4
Muon PID efficiency	2.3
Trigger efficiency	1.0
Fraction of J/ψ from b-hadron candidates	1.0
$\mathcal{B}(J/\psi \to \mu^+ \mu^-)$	1.1
Luminosity	3.9
Total	6.1

Table 1. Summary of the systematic uncertainties on the measurement of the J/ψ pair production cross-section.

the J/ψ pair production cross-section changes by $\pm 7\%$. The ratio of the production cross-section of the J/ψ pair to that of the inclusive prompt J/ψ is calculated to be

$$\frac{\sigma(J/\psi\,J/\psi)}{\sigma(J/\psi)} = (10.2 \pm 0.7\,(\text{stat}) \pm 0.9\,(\text{syst})) \times 10^{-4}, \qquad (5.1)$$

where the production cross-section of prompt J/ψ mesons in the range $2.0 < y < 4.5$ and $p_{\text{T}} < 10\,\text{GeV}/c$ is $\sigma(J/\psi) = 14.94 \pm 0.02\,(\text{stat}) \pm 0.91\,(\text{syst})\,\mu\text{b}$ [85], and the systematic uncertainties of $\sigma(J/\psi\,J/\psi)$ and $\sigma(J/\psi)$ are treated as uncorrelated. According to eq. (1.1), the ratio

$$\frac{1}{2}\frac{\sigma(J/\psi)^2}{\sigma(J/\psi\,J/\psi)} = 7.3 \pm 0.5\,(\text{stat}) \pm 1.0\,(\text{syst})\,\text{mb}. \qquad (5.2)$$

can be interpreted as σ_{eff} if all J/ψ pairs are produced through the DPS process.

The results on J/ψ pair production are compared with a data-driven prediction for the DPS mechanism and several calculations performed within the SPS mechanism. The DPS prediction is calculated via eq. (1.1) using the measured J/ψ production cross-section at $\sqrt{s} = 13\,\text{TeV}$ [85] and the effective cross-section $\sigma_{\text{eff}} = 14.5 \pm 1.7^{+1.7}_{-2.3}\,\text{mb}$ from refs. [44, 91].

Theoretical predictions of the production cross-section of J/ψ pairs are summarized in table 2. The contribution from the SPS mechanism is calculated using several approaches: the state-of-art complete NLO colour-singlet (NLO CS) computations [39]; the incomplete (no-loops) next-to-leading-order colour-singlet (NLO* CS) calculations [70, 92–96]; leading-order colour-singlet (LO CS) [92] and colour-octet (LO CO) [95, 96] calculations and the approach based on the k_{T}-factorisation method [97–101], with the leading-order colour-singlet matrix element (LO k_{T}) [102, 103]. Even with the leading-order matrix element, the LO k_{T} approach includes a large fraction of higher-order contributions via the evolution of parton densities [102]. Since NLO* CS calculations are divergent at small transverse momentum of the J/ψ pair, two approaches are used: a simple cut-off for $p_{\text{T}}(J/\psi\,J/\psi)$ [92] (denoted as NLO* CS$'$), and a cut on the mass of any light parton pair (NLO* CS$''$) [70, 93–96].

	$\sigma(J/\psi\,J/\psi)$ [nb]		
	no p_{T} cut	$p_{\mathrm{T}} > 1\,\mathrm{GeV}/c$	$p_{\mathrm{T}} > 3\,\mathrm{GeV}/c$
LO CS [92]	$1.3 \pm 0.1^{+3.2}_{-0.1}$	—	—
LO CO [95, 96]	$0.45 \pm 0.09^{+1.42+0.25}_{-0.36-0.34}$	—	—
LO k_{T} [102]	$6.3^{+3.8+3.8}_{-1.6-2.6}$	$5.7^{+3.4+3.2}_{-1.5-2.1}$	$2.7^{+1.6+1.6}_{-0.7-1.0}$
NLO* CS$'$ [92]	—	$4.3 \pm 0.1^{+9.9}_{-0.9}$	$1.6 \pm 0.1^{+3.3}_{-0.3}$
NLO* CS$''$ [70, 93–96]	$15.4 \pm 2.2^{+51}_{-12}$	$14.8 \pm 1.7^{+53}_{-12}$	$6.8 \pm 0.6^{+22}_{-5}$
NLO CS [39]	$11.9^{+4.6}_{-3.2}$	—	—
DPS [44, 85, 91]	$8.1 \pm 0.9^{+1.6}_{-1.3}$	$7.5 \pm 0.8^{+1.5}_{-1.2}$	$4.9 \pm 0.5^{+1.0}_{-0.8}$
Data	$15.2 \pm 1.0 \pm 0.9$	$13.5 \pm 0.9 \pm 0.9$	$8.3 \pm 0.6 \pm 0.5$

Table 2. Summary of the theoretical predictions and the measurement of $\sigma(J/\psi\,J/\psi)$ for different regions of transverse momentum of the J/ψ pair. For SPS predictions, the first uncertainty accounts for the variation of PDFs and gluon densities, while the second one corresponds to the variation of the factorisation and renormalisation scales. For the LO CO predictions the third uncertainty corresponds to the choice of LDMEs from refs. [25, 113–119]. For NLO CS predictions [39] the uncertainty corresponds to the variation of the factorisation and renormalization scales. For the DPS prediction the first uncertainty is due to the measured prompt J/ψ production cross-section [85] and the second is due to the uncertainty in σ_{eff} [44, 91].

Gluon densities from refs. [104–108] are used for the LO k_{T} approach, while CT 14 parton distribution functions (PDF) [109] are used for LO CS and NLO* CS$'$ calculations, NNPDF 3.0 NLO PDFs with $\alpha_s(M_Z) = 0.118$ [110] are used for LO CO and NLO* CS$''$ predictions, and CTEQ6L1 and CTEQ6M PDFs [111, 112] are used for NLO CS computations. For LO CO predictions the long-distance matrix elements (LDMEs) are taken from refs. [25, 113–119] and a smearing of transverse momenta of initial gluons, similar to that used in NLO* CS$''$, is applied. The production cross-section of J/ψ pairs is sensitive to the choice of parameters; for example, it varies by a factor between 0.8 and 3 when varying the factorisation and renormalisation scales by a factor of two, or increases if the CTEQ 6L PDF set [120] is used instead of the nominal PDFs. The contribution of LO CO is very sensitive to the choice of the LDME; the absolute cross-section varies from the minimum of 0.11 nb, based on LDME set from ref. [113] to the maximum of 0.70 nb, calculated using LDME set from ref. [116], while most of the predictions cluster around 0.5 nb. The feed-down from $\psi(2S) \to J/\psi\,X$ decays is included in the LO k_{T}, LO CO and NLO* CS$''$ calculations and not in the LO CS and NLO* CS$'$ calculations. Likewise, a tiny contribution from $J/\psi\,\chi_c$ production with subsequent decay $\chi_c \to J/\psi\,\gamma$ [92] is included in the NLO* CS$'$ and LO CO results but neglected in the NLO* CS$''$ calculations.

While the predictions for the production cross-section of J/ψ pairs are significantly affected by the theory uncertainties, the shapes of the differential cross-sections are very stable and practically invariant with respect to the choice of PDFs, scales and LDMEs.
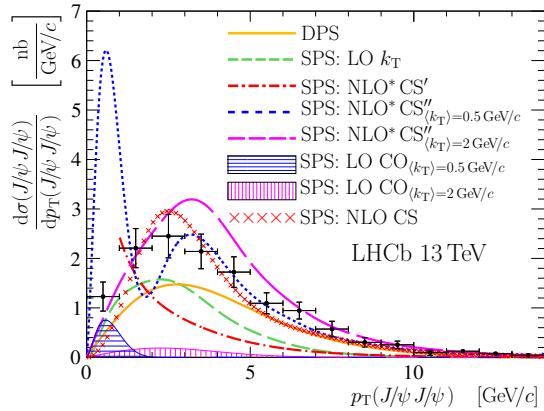
Figure 2. Comparisons between measurements and theoretical predictions for the differential cross-sections as a function of $p_{\mathrm{T}}(J/\psi\, J/\psi)$. The (black) points with error bars represent the measurements.

In contrast, the smearing of gluon transverse momenta for $\mathrm{NLO}^* \mathrm{CS}''$ and $\mathrm{LO\,CO}$ models does not affect the production cross-section, but significantly affects some differential distributions.

The measured differential production cross-sections of J/ψ pairs as a function of several kinematic variables are compared to the theoretical predictions. For each variable v, the differential production cross-section of J/ψ pairs is calculated as

$$\frac{\mathrm{d}\sigma(J/\psi\, J/\psi)}{\mathrm{d}v} = \frac{1}{\mathcal{L} \times \mathcal{B}(J/\psi \to \mu^+\mu^-)^2} \times \frac{\Delta N_i^{\mathrm{cor}}}{\Delta v_i},$$

where $\Delta N_i^{\mathrm{cor}}$ is the number of efficiency-corrected signal candidates in bin i, and Δv_i is the corresponding bin width. The luminosity uncertainty and the uncertainty introduced by $\mathcal{B}(J/\psi \to \mu^+\mu^-)$ are common to all bins and are fully correlated. The tracking efficiency and muon PID efficiency uncertainties are strongly correlated. In figures 2–8 of the differential cross-sections, only the statistical uncertainties are shown as the systematic ones are negligibly small and almost 100% correlated.

The comparison between measurements and theoretical predictions is performed for the following kinematical variables: transverse momentum and rapidity of the J/ψ pair, transverse momentum and rapidity of each J/ψ meson, differences in the azimuthal angle and rapidity between the two J/ψ mesons ($|\Delta\phi|$ and $|\Delta y|$), the mass of the J/ψ pair and the transverse momentum asymmetry, defined as

$$\mathcal{A}_{\mathrm{T}} \equiv \left| \frac{p_{\mathrm{T}}(J/\psi_1) - p_{\mathrm{T}}(J/\psi_2)}{p_{\mathrm{T}}(J/\psi_1) + p_{\mathrm{T}}(J/\psi_2)} \right|.$$

The distributions for the whole $p_{\mathrm{T}}(J/\psi\, J/\psi)$ range are presented in figures 2, 3 and 4, for $p_{\mathrm{T}}(J/\psi\, J/\psi) > 1\,\mathrm{GeV}/c$ in figures 5 and 6, and for $p_{\mathrm{T}}(J/\psi\, J/\psi) > 3\,\mathrm{GeV}/c$ in figures 7 and 8.

The DPS predictions are obtained using a large number of pseudoexperiments, where two uncorrelated J/ψ mesons are produced according to the measured differential distributions $\mathrm{d}^2\sigma\,(J/\psi)\,/\mathrm{d}p_{\mathrm{T}}\mathrm{d}y$ [85] for single prompt J/ψ production, uniformly distributed over
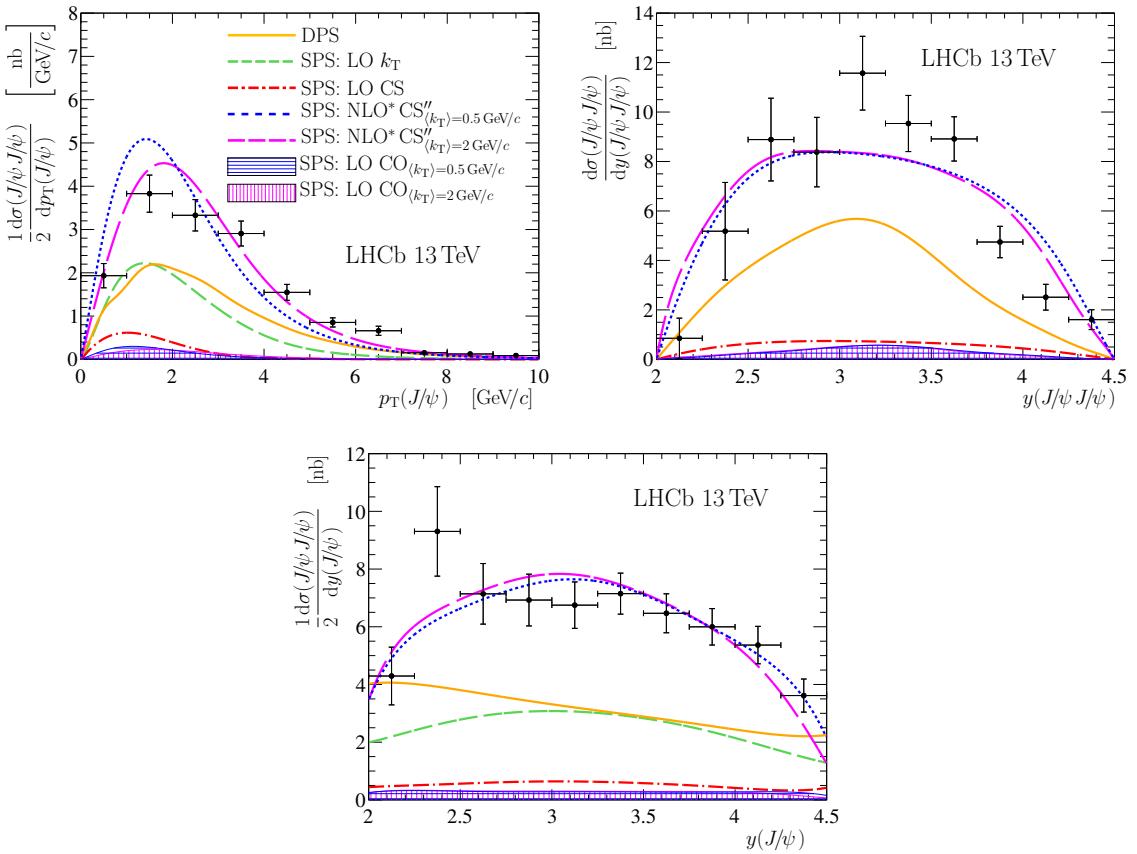
Figure 3. Comparisons between measurements and theoretical predictions for the differential cross-sections as functions of (top left) $p_{\rm T}(J/\psi)$, (top right) $y(J/\psi\,J/\psi)$ and (bottom) $y(J/\psi)$. The (black) points with error bars represent the measurements.

the azimuthal angle ϕ. For LO CO and NLO* CS$''$ models two values of Gaussian smearing of the initial transverse momentum of gluon $k_{\rm T}$ are used, namely $\langle k_{\rm T}\rangle = 0.5$ and $2\,{\rm GeV}/c$. The $p_{\rm T}(J/\psi\,J/\psi)$ distribution, shown in figure 2, demonstrates the large dependence of the shape on the choice of the $\langle k_{\rm T}\rangle$ parameter. For the NLO* CS$''$ approach [70, 93–96], relatively large smearing of the initial gluon transverse momenta $\langle k_{\rm T}\rangle = 2\,{\rm GeV}/c$ is required to eliminate peaking structures in the distribution. The distributions of the variables $p_{\rm T}(J/\psi\,J/\psi)$, $|\Delta\phi|$ and $\mathcal{A}_{\rm T}$, predicted by the LO CS model, are trivial, $p_{\rm T}(J/\psi\,J/\psi) \sim 0$, $|\Delta\phi| \sim \pi$ and $\mathcal{A}_{\rm T} \sim 0$, and omitted from the plots. A similar trivial pattern is expected for the LO CO model, but due to the $k_{\rm T}$-smearing, the actual shape of the distributions strongly depends on the choice of the $\langle k_{\rm T}\rangle$ parameter. The NLO* CS$''$ model also demonstrates a large dependence on the $\langle k_{\rm T}\rangle$ parameter for $|\Delta\phi|/\pi$ distribution.

Neither the DPS model with the given value of the $\sigma_{\rm eff}$ parameter, nor any of the SPS models can describe simultaneously the measured cross-section and the differential shapes. However, the sum of the DPS and SPS contributions can adequately describe both the measured production cross-sections and the differential distributions. To discriminate between the SPS and DPS contributions, the differential distribution for each variable v is
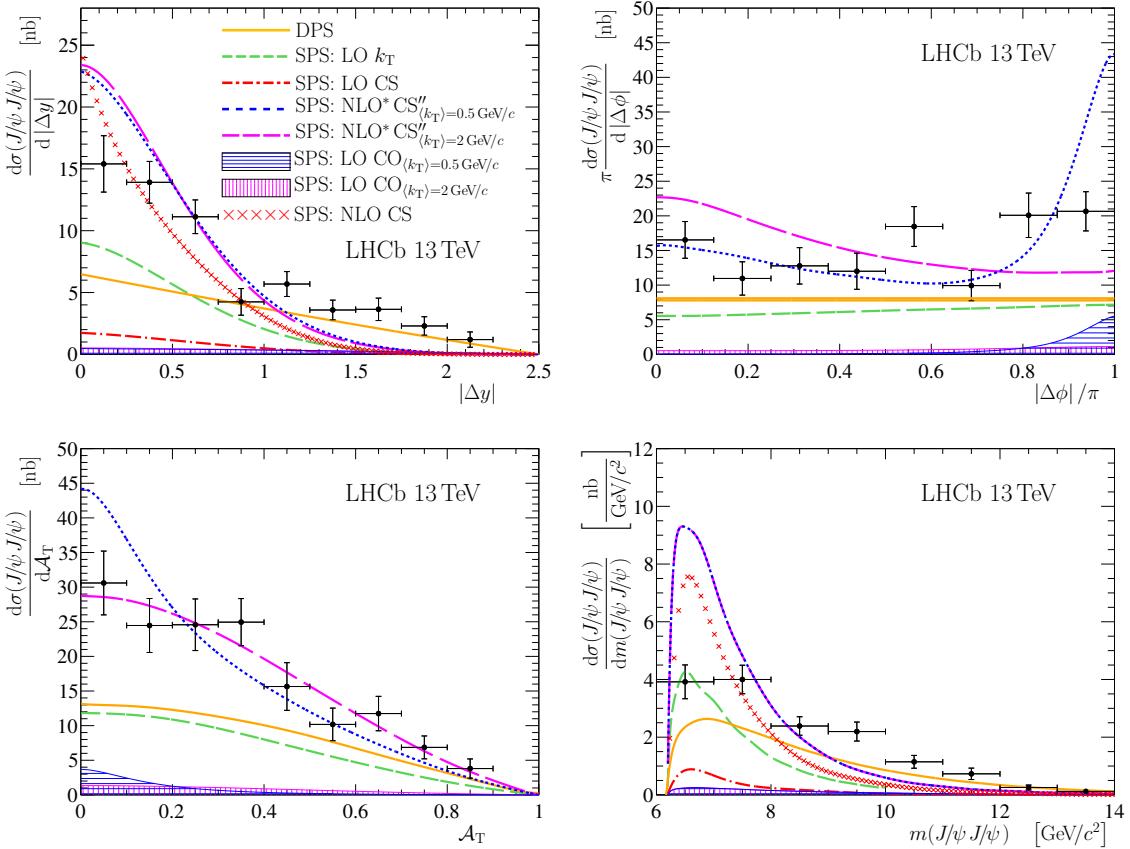
Figure 4. Comparisons between measurements and theoretical predictions for the differential cross-sections as functions of (top left) $|\Delta y|$, (top right) $|\Delta \phi|$, (bottom left) $\mathcal{A}_{\mathrm{T}}$ and (bottom right) $m(J/\psi\,J/\psi)$. The (black) points with error bars represent the measurements.

fitted with the simple two-component model

$$\frac{\mathrm{d}\sigma}{\mathrm{d}v} = \sigma_{\mathrm{DPS}}F_{\mathrm{DPS}}(v) + \sigma_{\mathrm{SPS}}F_{\mathrm{SPS}}(v), \tag{5.3}$$

where F_{DPS} and F_{SPS} are templates for the DPS and SPS models and σ_{DPS} and σ_{SPS} are floating fit parameters representing the DPS and SPS contributions. The theory normalisation is not used in the fits. The DPS fraction f_{DPS} is defined as

$$f_{\mathrm{DPS}} \equiv \frac{\sigma_{\mathrm{DPS}}}{\sigma_{\mathrm{SPS}} + \sigma_{\mathrm{DPS}}}. \tag{5.4}$$

Some distributions give little discrimination between SPS and DPS. The percentages of the DPS component obtained from the fits for the most discriminating variables are presented in table 3. The fit results are presented in the appendix. All the fits indicate a large DPS contribution to the J/ψ pair production process. The inclusion of the CO component in the fit does not have a large effect on the determination of the DPS fraction f_{DPS}, and the fraction of the CO component determined in such a fit procedure is significantly smaller than the CS contribution. The value of σ_{SPS}, calculated as $(1 - f_{\mathrm{DPS}}) \times \sigma(J/\psi\,J/\psi)$,
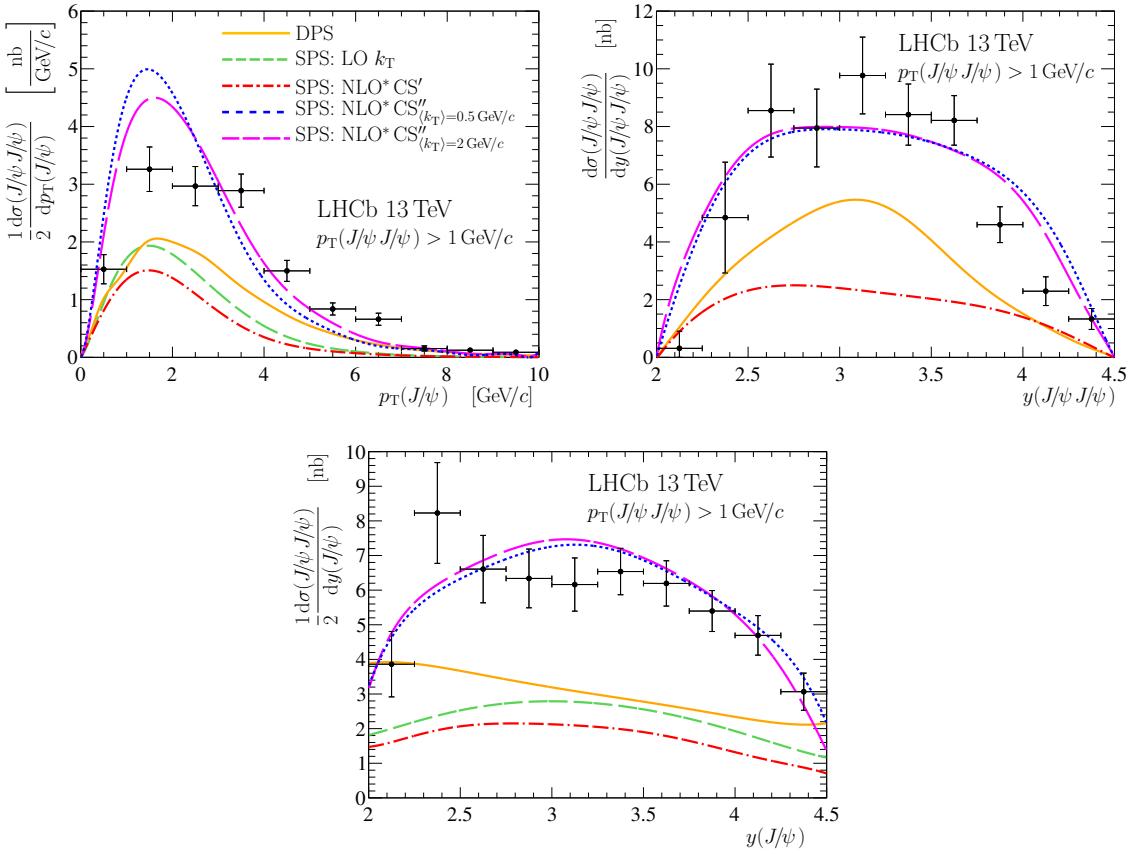
Figure 5. Comparisons between measurements and theoretical predictions with $p_{\mathrm{T}}(J/\psi\,J/\psi) > 1\,\mathrm{GeV}/c$ for the differential cross-sections as functions of (top left) $p_{\mathrm{T}}(J/\psi)$, (top right) $y(J/\psi\,J/\psi)$ and (bottom) $y(J/\psi)$. The (black) points with error bars represent the measurements.

is smaller than expectations from the $\mathrm{NLO^* CS''}$ [70, 93–96] and NLO CS [39] approaches and roughly agrees with the $\mathrm{NLO^* CS'}$ [92] and LO k_{T} [102] predictions.

The value σ_{DPS} determined with eq. (5.3) is converted to σ_{eff},

$$\sigma_{\mathrm{eff}} = \frac{1}{2}\frac{\sigma\left(J/\psi\right)^2}{\sigma_{\mathrm{DPS}}}, \tag{5.5}$$

where $\sigma(J/\psi)$ is the production cross-section of prompt J/ψ mesons from ref. [85]. The values obtained for σ_{eff} are summarized in table 4. Values between 10.0 and 12.5 mb are found for the models considered in this analysis. These values are slightly larger than those measured from central J/ψ pair production at LHC, $\sigma_{\mathrm{eff}} = 8.2 \pm 2.2\,\mathrm{mb}$ [70] and $\sigma_{\mathrm{eff}} = 6.3 \pm 1.9\,\mathrm{mb}$ [59], and significantly exceed the values obtained by the D0 collaboration from analysis of J/ψ pair production, $\sigma_{\mathrm{eff}} = 4.8 \pm 2.5\,\mathrm{mb}$ [60], and $\Upsilon J/\psi$ production, $\sigma_{\mathrm{eff}} = 2.2 \pm 1.1\,\mathrm{mb}$ [71]. On the other hand, they are smaller than the values of σ_{eff} measured by the LHCb collaboration in the processes of multiple associated heavy quark production [52, 54], in particular $\sigma_{\mathrm{eff}} \sim 15\,\mathrm{mb}$ measured for various $J/\psi + c\bar{c}$ production processes [52] and $\sigma_{\mathrm{eff}} = 18.0 \pm 1.8\,\mathrm{mb}$ measured for the $\Upsilon(1S) + D^{0,+}$ production processes [54].

Variable	LO CS	LO k_{T}	NLO* CS′	NLO* CS″ $\langle k_{\mathrm{T}}\rangle = 2\,\mathrm{GeV}/c$	$\langle k_{\mathrm{T}}\rangle = 0.5\,\mathrm{GeV}/c$	NLO CS
				no $p_{\mathrm{T}}(J/\psi\,J/\psi)$ cut		
$p_{\mathrm{T}}(J/\psi\,J/\psi)$	—	78 ± 3	—	88 ± 56	81 ± 7	—
$y(J/\psi\,J/\psi)$	83 ± 39	—	—	75 ± 37	68 ± 34	—
$m(J/\psi\,J/\psi)$	76 ± 7	74 ± 7	—	78 ± 7		77 ± 7
$|\Delta y|$	59 ± 21	61 ± 18	—	63 ± 18	61 ± 18	69 ± 16
				$p_{\mathrm{T}}(J/\psi\,J/\psi) > 1\,\mathrm{GeV}/c$		
$y(J/\psi\,J/\psi)$	—	—	75 ± 24	71 ± 38	68 ± 34	—
$m(J/\psi\,J/\psi)$	—	73 ± 8	76 ± 7	88 ± 1		—
$|\Delta y|$	—	57 ± 20	59 ± 19	60 ± 18	60 ± 19	—
				$p_{\mathrm{T}}(J/\psi\,J/\psi) > 3\,\mathrm{GeV}/c$		
$y(J/\psi\,J/\psi)$	—	—	77 ± 18	64 ± 38	64 ± 35	—
$m(J/\psi\,J/\psi)$	—	76 ± 10	84 ± 7	87 ± 2		—
$|\Delta y|$	—	42 ± 25	53 ± 21	53 ± 21	53 ± 21	—

Table 3. Percentages of the DPS component, f_{DPS}, determined with the simple two-component fit to different distributions for different SPS models.

Variable	LO k_{T}	NLO* CS″ $\langle k_{\mathrm{T}}\rangle = 2\,\mathrm{GeV}/c$	$\langle k_{\mathrm{T}}\rangle = 0.5\,\mathrm{GeV}/c$	NLO CS
$p_{\mathrm{T}}(J/\psi\,J/\psi)$	11.3 ± 0.6	10.1 ± 6.5	10.9 ± 1.2	—
$y(J/\psi\,J/\psi)$	—	11.9 ± 7.5	10.0 ± 5.0	—
$m(J/\psi\,J/\psi)$	10.6 ± 1.1	10.2 ± 1.0		10.4 ± 1.0
$|\Delta y|$	12.5 ± 4.1	12.2 ± 3.7	12.4 ± 3.9	11.2 ± 2.9

Table 4. Summary of the σ_{eff} values (in mb) from DPS fits for different SPS models. The uncertainty is statistical only, originating from the statistical uncertainty in σ_{DPS} (and $\mathrm{d}\sigma(J/\psi\,J/\psi)/\mathrm{d}v$). The common systematic uncertainty of 12%, accounting for the systematic uncertainty of $\sigma(J/\psi\,J/\psi)$ and the total uncertainty for $\sigma(J/\psi)$, is not shown.
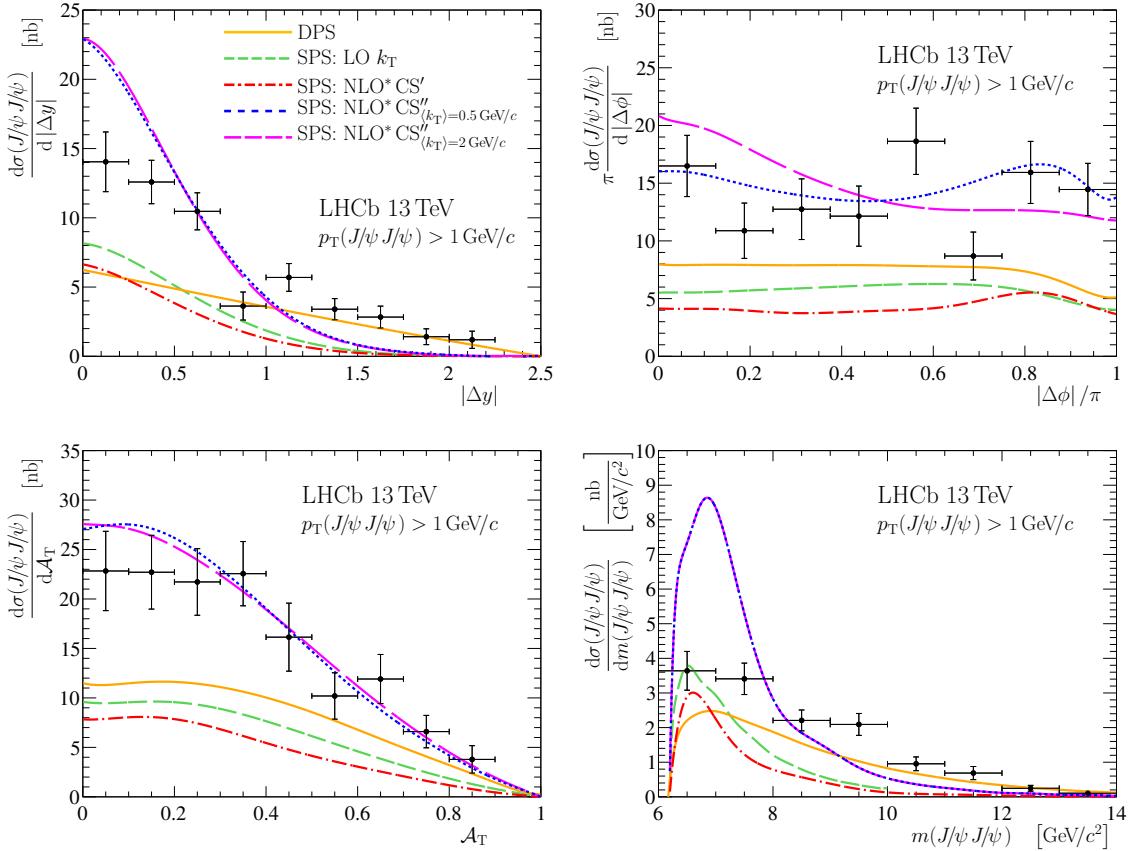
Figure 6. Comparisons between measurements and theoretical predictions with $p_{\mathrm{T}}(J/\psi\,J/\psi) > 1\,\mathrm{GeV}/c$ for the differential cross-sections as functions of (top left) $|\Delta y|$, (top right) $|\Delta\phi|$, (bottom left) $\mathcal{A}_{\mathrm{T}}$ and (bottom right) $m(J/\psi\,J/\psi)$. The (black) points with error bars represent the measurements.
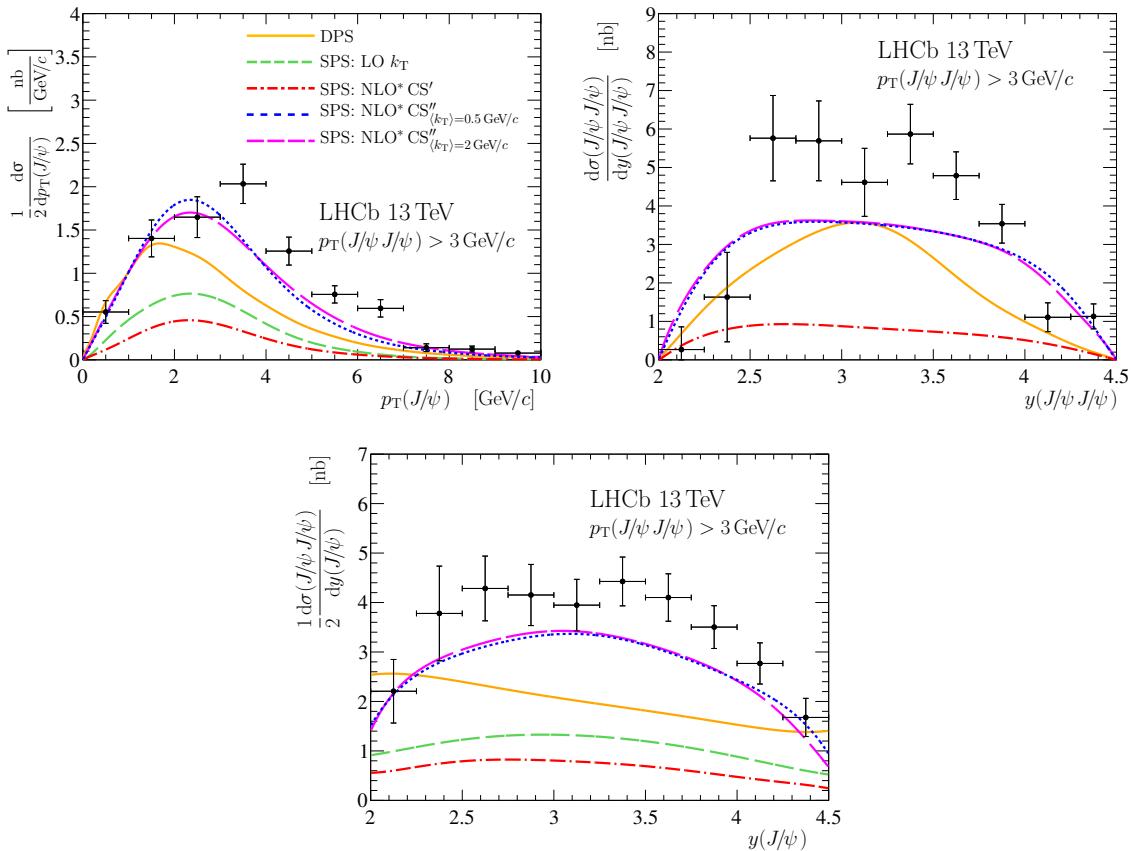
Figure 7. Comparisons between measurements and theoretical predictions with $p_T(J/\psi\,J/\psi) > 3\,\text{GeV}/c$ for the differential cross-sections as functions of (top left) $p_T(J/\psi)$, (top right) $y(J/\psi\,J/\psi)$ and (bottom) $y(J/\psi)$. The (black) points with error bars represent the measurements.
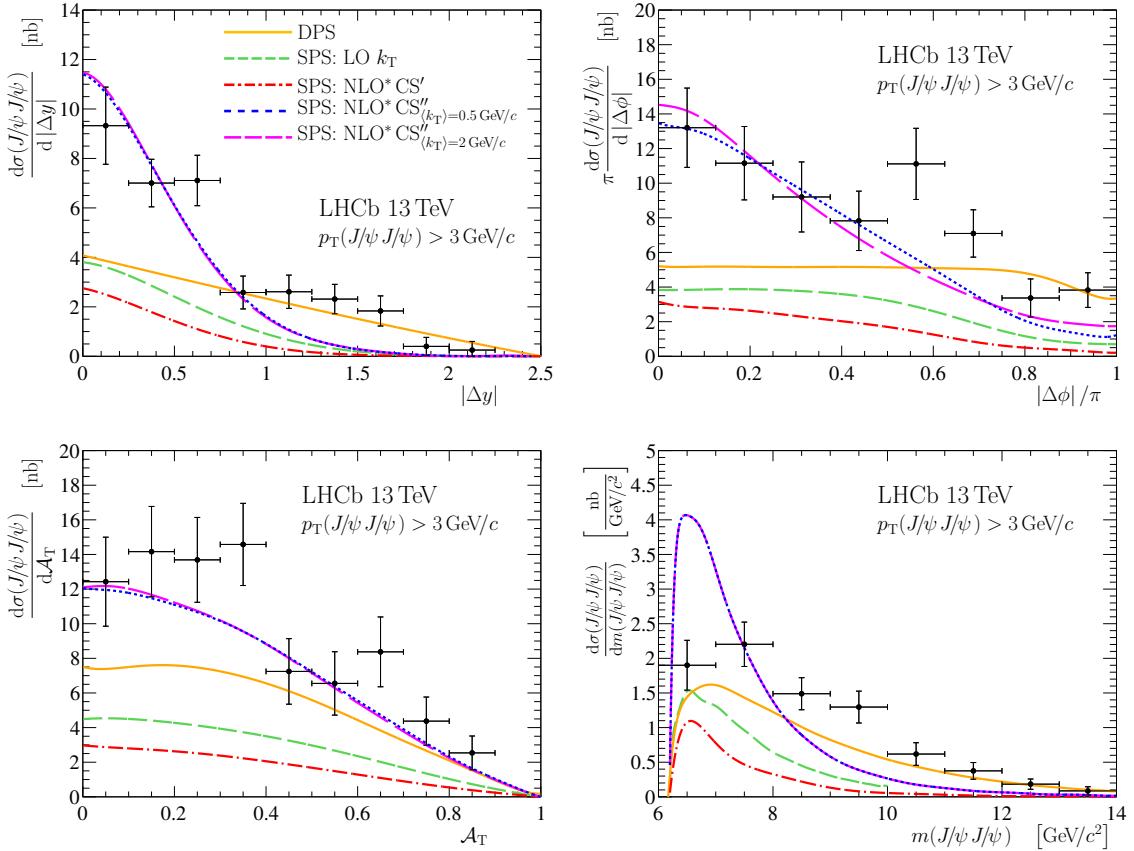
Figure 8. Comparisons between measurements and theoretical predictions with $p_T(J/\psi\,J/\psi) > 3\,\mathrm{GeV}/c$ for the differential cross-sections as functions of (top left) $|\Delta y|$, (top right) $|\Delta\phi|$, (bottom left) $\mathcal{A}_T$ and (bottom right) $m(J/\psi\,J/\psi)$. The (black) points with error bars represent the measurements.

6 Summary

The J/ψ pair production cross-section with both J/ψ mesons in the region $2.0 < y < 4.5$ and $p_{\mathrm{T}} < 10\,\mathrm{GeV}/c$ is measured to be $15.2 \pm 1.0\,(\mathrm{stat}) \pm 0.9\,(\mathrm{syst})\,\mathrm{nb}$, using pp collision data collected by LHCb at $\sqrt{s} = 13\,\mathrm{TeV}$, corresponding to an integrated luminosity of $279\,\mathrm{pb}^{-1}$. The differential production cross-sections as functions of $p_{\mathrm{T}}(J/\psi\,J/\psi)$, $p_{\mathrm{T}}(J/\psi)$, $m(J/\psi\,J/\psi)$, $y(J/\psi\,J/\psi)$, $y(J/\psi)$, $|\Delta\phi|$, $|\Delta y|$ and $\mathcal{A}_{\mathrm{T}}$ are compared to theoretical predictions. A fit to the differential cross-sections using simple DPS plus SPS models indicates a significant DPS contribution. The data can be reasonably well described with a sum of DPS and SPS colour-singlet contributions, with no evidence for a large SPS colour-octet contribution. The obtained SPS contribution is overestimated in the $\mathrm{NLO^*\,CS''}$ [70, 93–96] and $\mathrm{NLO\,CS}$ [39] approaches and roughly agrees with the $\mathrm{NLO^*\,CS'}$ [92] and $\mathrm{LO}\,k_{\mathrm{T}}$ [102] predictions. Good agreement with the data for the differential cross-sections calculated within the $\mathrm{LO}\,k_{\mathrm{T}}$ [102] and $\mathrm{NLO^*\,CS'}$ [92] approaches indicates that a significant part of high-order contributions can be properly accounted via the evolution of parton densities [102]. Relatively large smearing of initial gluon transverse momenta $\langle k_{\mathrm{T}} \rangle = 2\,\mathrm{GeV}/c$ is preferred over $\langle k_{\mathrm{T}} \rangle = 0.5\,\mathrm{GeV}/c$ for the $\mathrm{NLO^*\,CS''}$ approach [70, 93–96]. An improvement in the precision for SPS predictions is needed for a better discrimination between the different theory approaches. A large DPS contribution results in values of σ_{eff} that are smaller than the values of σ_{eff} measured previously by the LHCb collaboration in the processes of multiple associated heavy quark production [52, 54], and slightly larger than those measured from central J/ψ pair production at the CMS [58] and ATLAS [59] experiments.

A   Fits to the differential cross-sections with SPS and DPS components

The results of fits used for the determination of σ_{eff} are shown in figures 9, 10 and 11. The fits used only for determination of f_{DPS} in $p_{\text{T}}(J/\psi\,J/\psi) > 1\,\text{GeV}/c$ and $p_{\text{T}}(J/\psi\,J/\psi) > 3\,\text{GeV}/c$ regions are shown in figures 12, 13, 14 and 15.
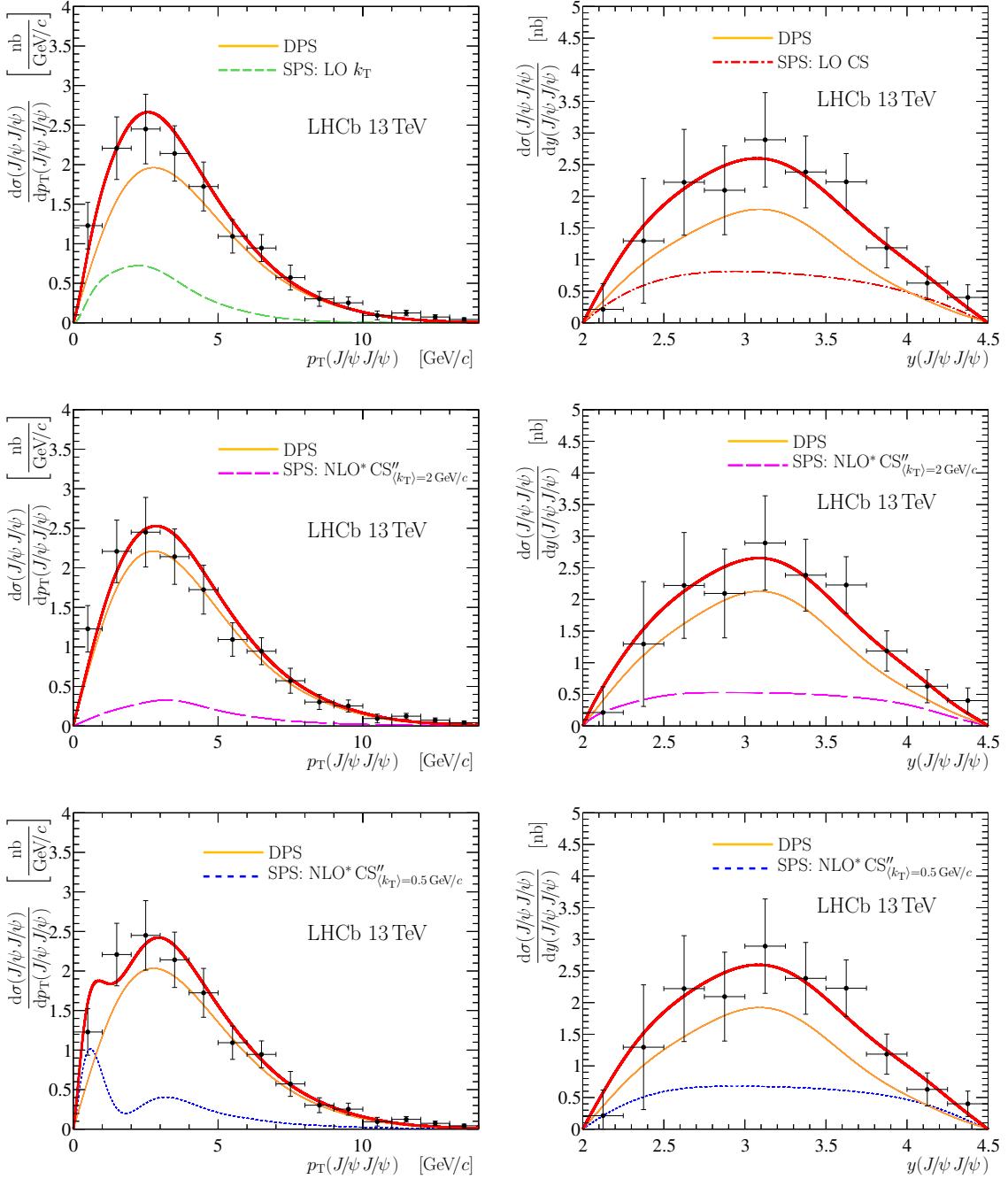
Figure 9. Result of templated DPS fit for $\frac{\mathrm{d}\sigma(J/\psi\,J/\psi)}{\mathrm{d}p_{\mathrm{T}}(J/\psi\,J/\psi)}$ and $\frac{\mathrm{d}\sigma(J/\psi\,J/\psi)}{\mathrm{d}y(J/\psi\,J/\psi)}$. The (black) points with error bars represent the data. The total fit result is shown with the thick (red) solid line and the DPS component is shown with the thin (orange) solid line.
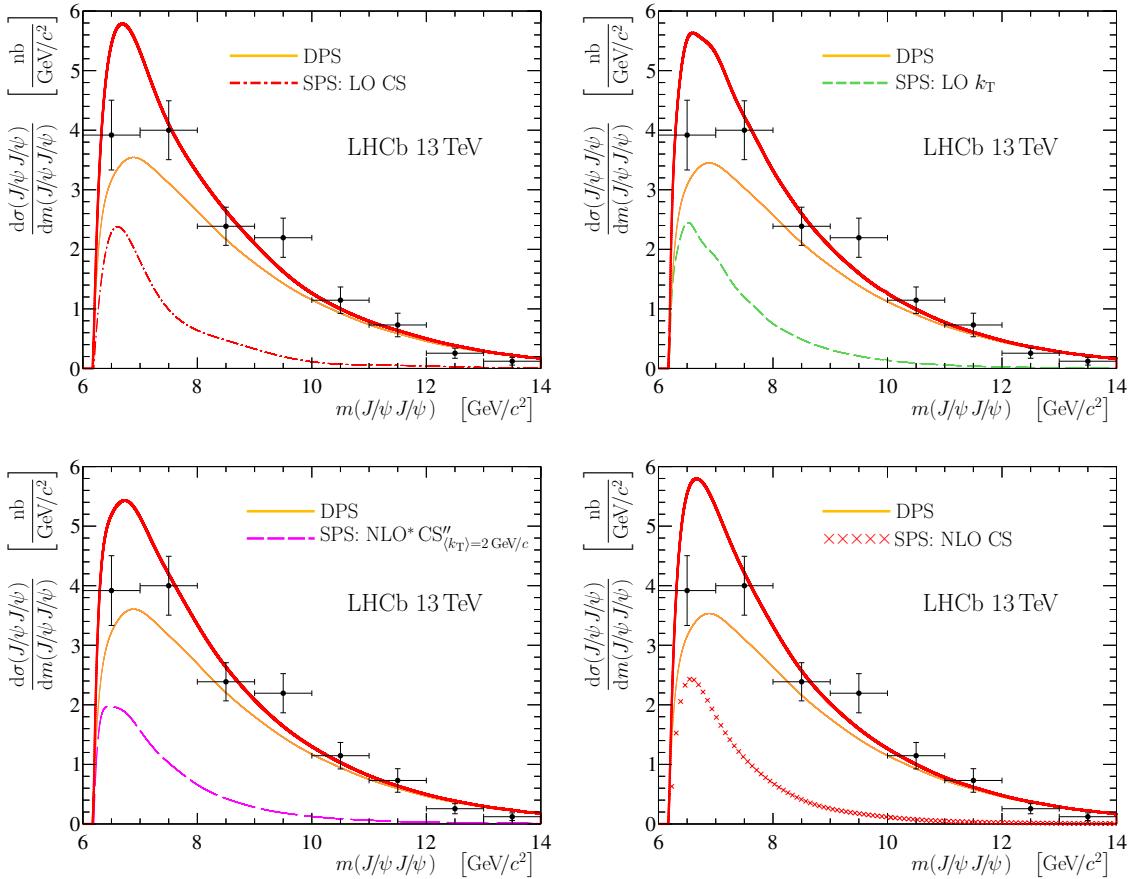
Figure 10. Result of templated DPS fit for $\frac{\mathrm{d}\sigma(J/\psi\,J/\psi)}{\mathrm{d}m(J/\psi\,J/\psi)}$. The (black) points with error bars represent the data. The total fit result is shown with the thick (red) solid line and the DPS component is shown with the thin (orange) solid line.
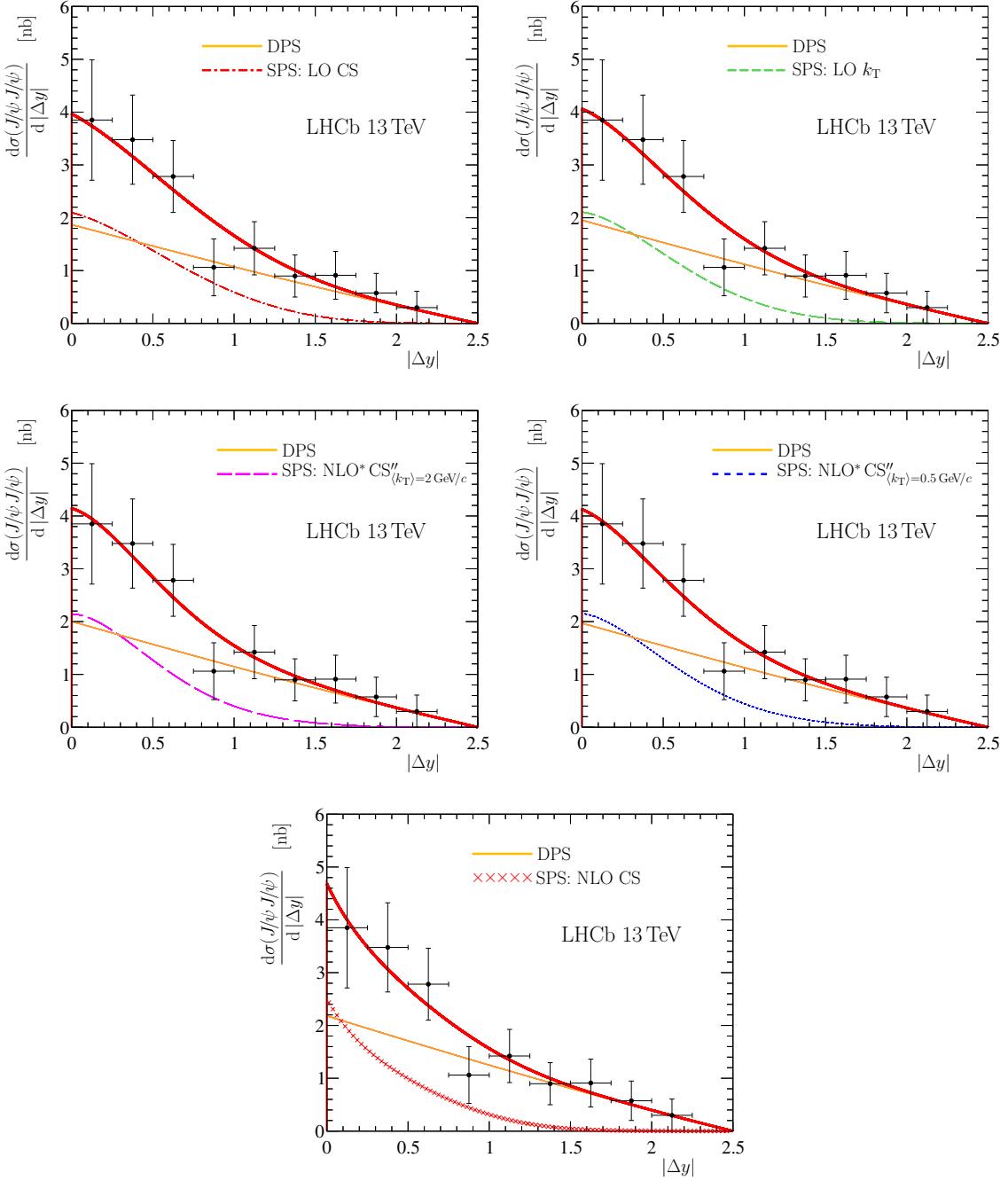
Figure 11. Result of templated DPS fit for $\frac{\mathrm{d}\sigma(J/\psi\,J/\psi)}{\mathrm{d}|\Delta y|}$. The (black) points with error bars represent the data. The total fit result is shown with the thick (red) solid line and the DPS component is shown with the thin (orange) solid line.
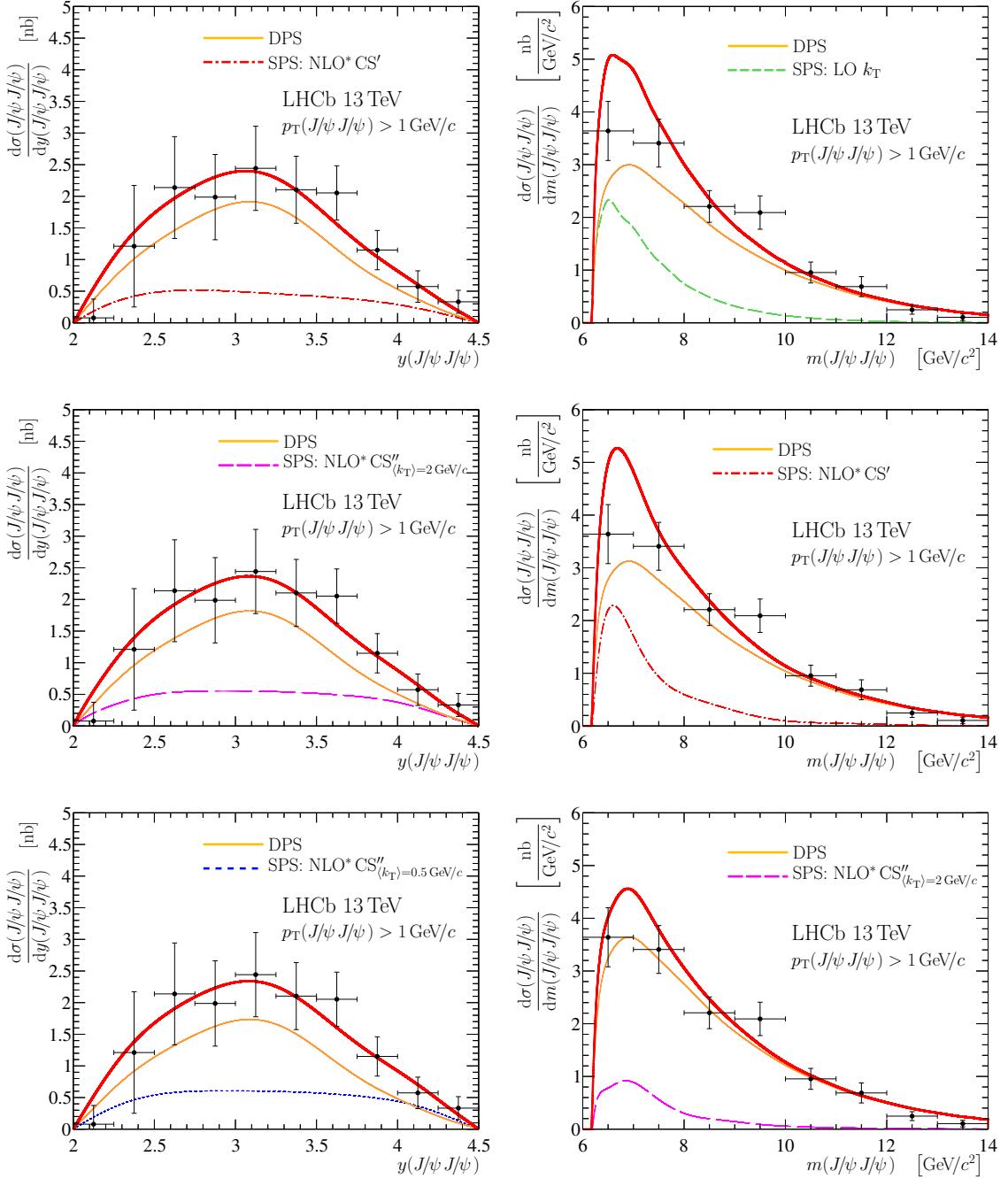
Figure 12. Result of templated DPS fit for $\frac{\mathrm{d}\sigma(J/\psi\,J/\psi)}{\mathrm{d}y(J/\psi\,J/\psi)}$ and $\frac{\mathrm{d}\sigma(J/\psi)}{\mathrm{d}m(J/\psi\,J/\psi)}$ for the $p_{\mathrm{T}}(J/\psi\,J/\psi) > 1\,\mathrm{GeV}/c$ region. The (black) points with error bars represent the data. The total fit result is shown with the thick (red) solid line and the DPS component is shown with the thin (orange) solid line.
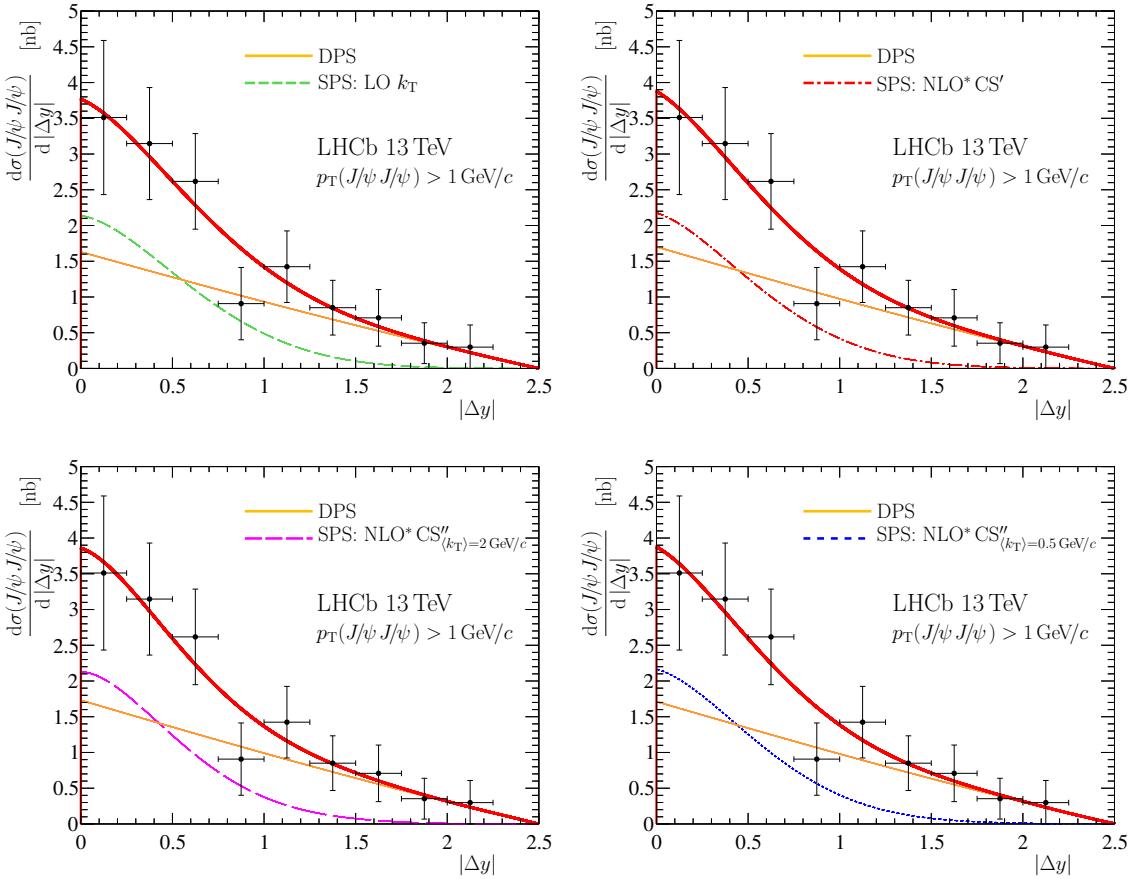
Figure 13. Result of templated DPS fit for $\frac{\mathrm{d}\sigma(J/\psi\,J/\psi)}{\mathrm{d}|\Delta y|}$ for the $p_\mathrm{T}(J/\psi\,J/\psi) > 1\,\mathrm{GeV}/c$ region. The (black) points with error bars represent the data. The total fit result is shown with the thick (red) solid line and the DPS component is shown with the thin (orange) solid line.
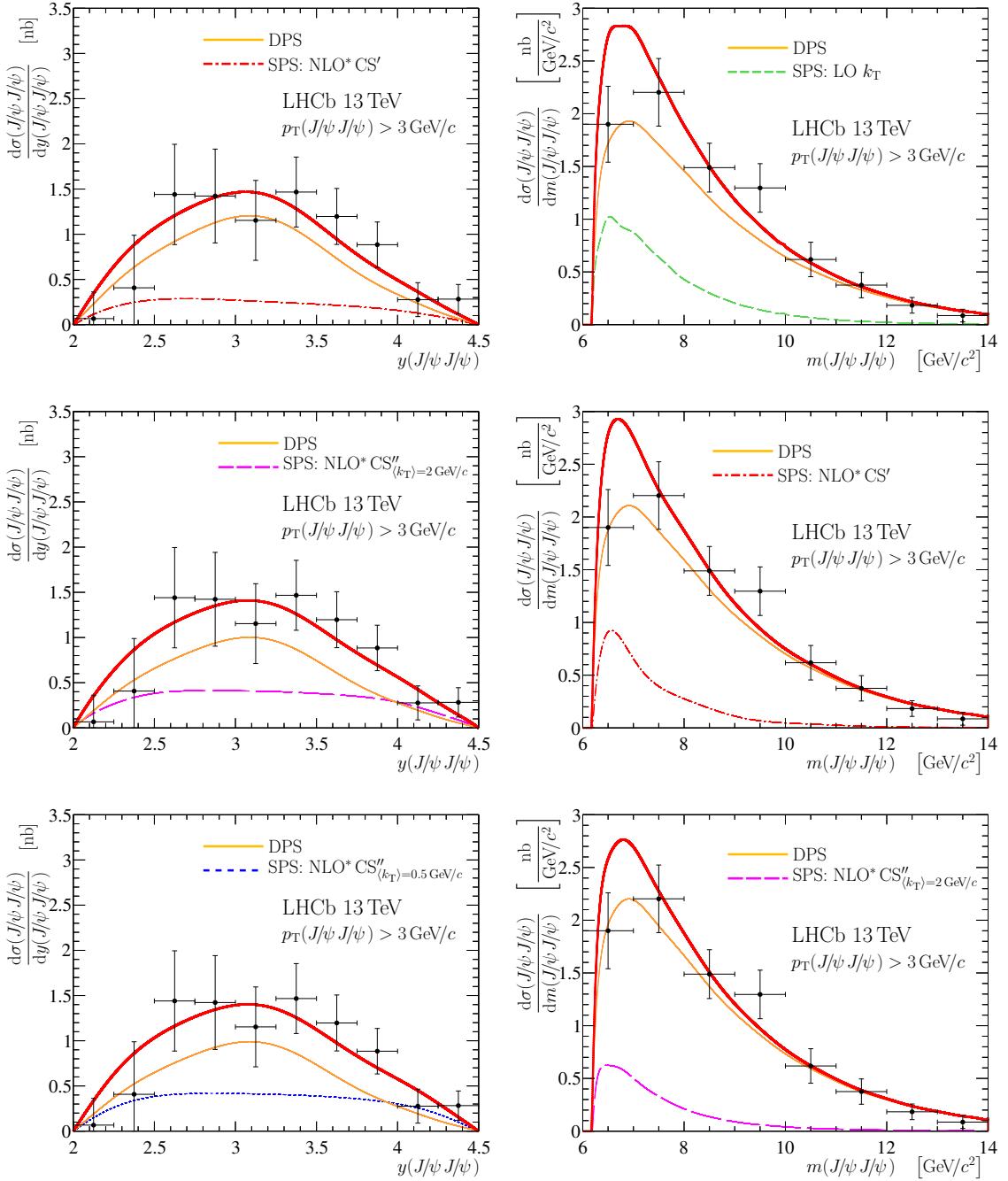
Figure 14. Result of templated DPS fit for $\frac{\mathrm{d}\sigma(J/\psi\,J/\psi)}{\mathrm{d}y(J/\psi\,J/\psi)}$ and $\frac{\mathrm{d}\sigma(J/\psi\,J/\psi)}{\mathrm{d}m(J/\psi\,J/\psi)}$ for the $p_{\mathrm{T}}(J/\psi\,J/\psi) > 3\,\mathrm{GeV}/c$ region. The (black) points with error bars represent the data. The total fit result is shown with the thick (red) solid line and the DPS component is shown with the thin (orange) solid line.
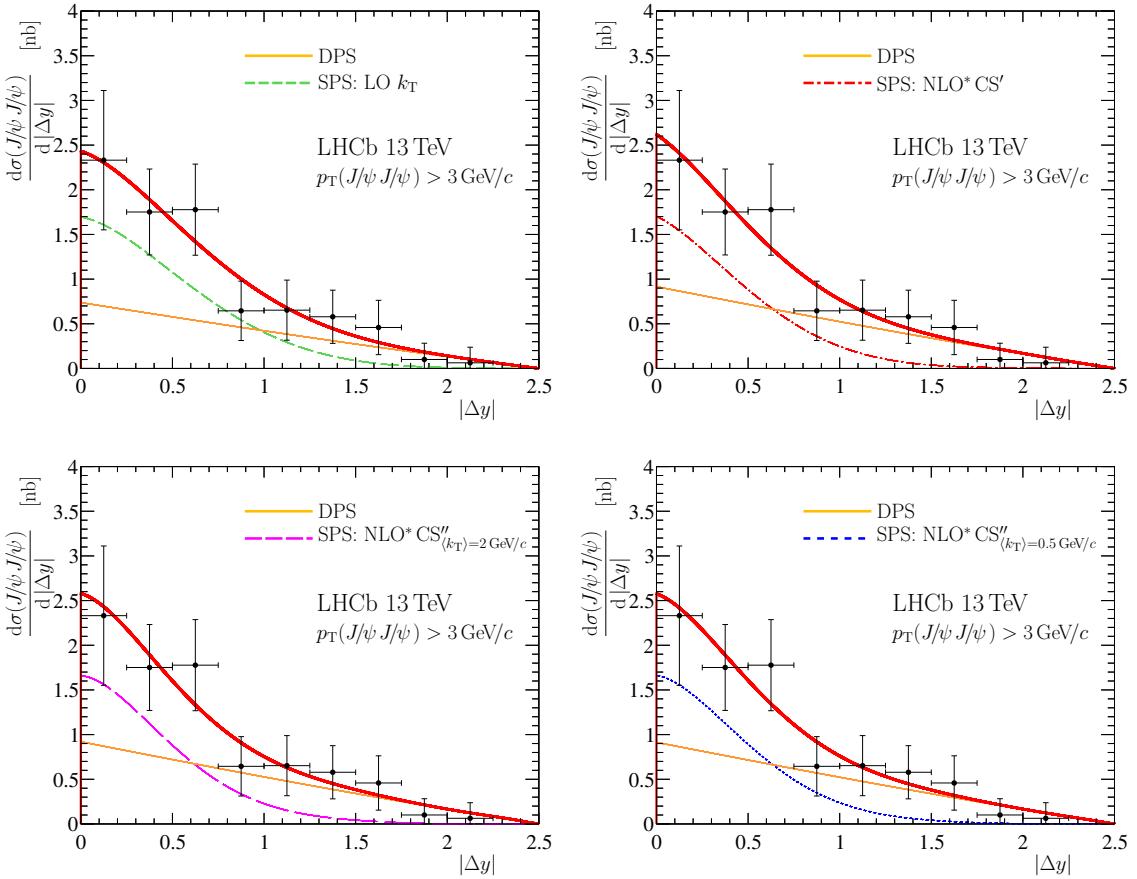
Figure 15. Result of templated DPS fit for $\frac{\mathrm{d}\sigma(J/\psi\,J/\psi)}{\mathrm{d}|\Delta y|}$ for the $p_{\mathrm{T}}(J/\psi\,J/\psi) > 3\,\mathrm{GeV}/c$ region. The (black) points with error bars represent the data. The total fit result is shown with the thick (red) solid line and the DPS component is shown with the thin (orange) solid line.

References

[1] C.E. Carlson and R. Suaya, *Hadronic production of ψ/J mesons*, *Phys. Rev.* **D 14** (1976) 3115 [ɪɴSPIRE].

[2] A. Donnachie and P.V. Landshoff, *Production of lepton pairs, J/ψ and charm with hadron beams*, *Nucl. Phys.* **B 112** (1976) 233 [ɪɴSPIRE].

[3] S.D. Ellis, M.B. Einhorn and C. Quigg, *Comment on hadronic production of psions*, *Phys. Rev. Lett.* **36** (1976) 1263 [ɪɴSPIRE].

[4] H. Fritzsch, *Producing heavy quark flavors in hadronic collisions: a test of quantum chromodynamics*, *Phys. Lett.* **B 67** (1977) 217 [ɪɴSPIRE].

[5] M. Glück, J.F. Owens and E. Reya, *Gluon contribution to hadronic J/ψ production*, *Phys. Rev.* **D 17** (1978) 2324 [ɪɴSPIRE].

[6] V.G. Kartvelishvili, A.K. Likhoded and S.R. Slabospitsky, *D meson and ψ meson production in hadronic interactions*, *Sov. J. Nucl. Phys.* **28** (1978) 678 [ɪɴSPIRE].

[7] V.G. Kartvelishvili, A.K. Likhoded and S.R. Slabospitsky, *On charmed particle hadronic production*, *Sov. J. Nucl. Phys.* **33** (1981) 434 [ɪɴSPIRE].

[8] E.L. Berger and D.L. Jones, *Inelastic photoproduction of J/ψ and Υ by gluons*, *Phys. Rev.* **D 23** (1981) 1521 [ɪɴSPIRE].

[9] C.-H. Chang, *Hadronic production of J/ψ associated with a gluon*, *Nucl. Phys.* **B 172** (1980) 425 [ɪɴSPIRE].

[10] R. Baier and R. Rückl, *Hadronic production of J/ψ and Υ: transverse momentum distributions*, *Phys. Lett.* **B 102** (1981) 364 [ɪɴSPIRE].

[11] CDF collaboration, F. Abe et al., *J/ψ and $\psi(2S)$ production in $p\bar{p}$ collisions at $\sqrt{s} = 1.8\ TeV$*, *Phys. Rev. Lett.* **79** (1997) 572 [ɪɴSPIRE].

[12] J.M. Campbell, F. Maltoni and F. Tramontano, *QCD corrections to J/ψ and Υ production at hadron colliders*, *Phys. Rev. Lett.* **98** (2007) 252002 [hep-ph/0703113] [ɪɴSPIRE].

[13] J.P. Lansberg, *J/ψ production at $\sqrt{s} = 1.96$ and $7\ TeV$: Color-Singlet Model, NNLO* and polarisation*, *J. Phys.* **G 38** (2011) 124110 [arXiv:1107.0292] [ɪɴSPIRE].

[14] B. Gong and J.-X. Wang, *Next-to-leading-order QCD corrections to J/ψ polarization at Tevatron and Large-Hadron-Collider energies*, *Phys. Rev. Lett.* **100** (2008) 232001 [arXiv:0802.3727] [ɪɴSPIRE].

[15] G.T. Bodwin, E. Braaten and G.P. Lepage, *Rigorous QCD analysis of inclusive annihilation and production of heavy quarkonium*, *Phys. Rev.* **D 51** (1995) 1125 [*Erratum ibid.* **D 55** (1997) 5853] [hep-ph/9407339] [ɪɴSPIRE].

[16] P.L. Cho and A.K. Leibovich, *Color octet quarkonia production*, *Phys. Rev.* **D 53** (1996) 150 [hep-ph/9505329] [ɪɴSPIRE].

[17] P.L. Cho and A.K. Leibovich, *Color octet quarkonia production. 2.*, *Phys. Rev.* **D 53** (1996) 6203 [hep-ph/9511315] [ɪɴSPIRE].

[18] M. Cacciari, M. Greco, M.L. Mangano and A. Petrelli, *Charmonium production at the Tevatron*, *Phys. Lett.* **B 356** (1995) 553 [hep-ph/9505379] [INSPIRE].

[19] E. Braaten and S. Fleming, *Color octet fragmentation and the ψ' surplus at the Tevatron*, *Phys. Rev. Lett.* **74** (1995) 3327 [hep-ph/9411365] [INSPIRE].

[20] Y.-Q. Ma, K. Wang and K.-T. Chao, *A complete NLO calculation of the J/ψ and ψ' production at hadron colliders*, *Phys. Rev.* **D 84** (2011) 114001 [arXiv:1012.1030] [INSPIRE].

[21] B. Gong, X.Q. Li and J.-X. Wang, *QCD corrections to J/ψ production via color octet states at Tevatron and LHC*, *Phys. Lett.* **B 673** (2009) 197 [*Erratum ibid.* **B 693** (2010) 612] [arXiv:0805.4751] [INSPIRE].

[22] M. Butenschoen and B.A. Kniehl, *Reconciling J/ψ production at HERA, RHIC, Tevatron and LHC with NRQCD factorization at next-to-leading order*, *Phys. Rev. Lett.* **106** (2011) 022003 [arXiv:1009.5662] [INSPIRE].

[23] M. Beneke and I.Z. Rothstein, *ψ' polarization as a test of color octet quarkonium production*, *Phys. Lett.* **B 372** (1996) 157 [*Erratum ibid.* **B 389** (1996) 769] [hep-ph/9509375] [INSPIRE].

[24] K.-T. Chao, Y.-Q. Ma, H.-S. Shao, K. Wang and Y.-J. Zhang, *J/ψ polarization at hadron colliders in nonrelativistic QCD*, *Phys. Rev. Lett.* **108** (2012) 242004 [arXiv:1201.2675] [INSPIRE].

[25] B. Gong, L.-P. Wan, J.-X. Wang and H.-F. Zhang, *Polarization for prompt J/ψ and $\psi(2s)$ production at the Tevatron and LHC*, *Phys. Rev. Lett.* **110** (2013) 042002 [arXiv:1205.6682] [INSPIRE].

[26] M. Butenschoen and B.A. Kniehl, *J/ψ polarization at Tevatron and LHC: nonrelativistic-QCD factorization at the crossroads*, *Phys. Rev. Lett.* **108** (2012) 172002 [arXiv:1201.1872] [INSPIRE].

[27] CDF collaboration, A. Abulencia et al., *Polarization of J/ψ and ψ_{2S} mesons produced in $p\bar{p}$ collisions at $\sqrt{s} = 1.96 - TeV$*, *Phys. Rev. Lett.* **99** (2007) 132001 [arXiv:0704.0638] [INSPIRE].

[28] D0 collaboration, V.M. Abazov et al., *Measurement of the polarization of the υ_{1S} and υ_{2S} states in $p\bar{p}$ collisions at $\sqrt{s} = 1.96\ TeV$*, *Phys. Rev. Lett.* **101** (2008) 182004 [arXiv:0804.2799] [INSPIRE].

[29] ALICE collaboration, *J/ψ polarization in pp collisions at $\sqrt{s} = 7\ TeV$*, *Phys. Rev. Lett.* **108** (2012) 082001 [arXiv:1111.1630] [INSPIRE].

[30] CMS collaboration, *Measurement of the prompt J/ψ and $\psi(2S)$ polarizations in pp collisions at $\sqrt{s} = 7\ TeV$*, *Phys. Lett.* **B 727** (2013) 381 [arXiv:1307.6070] [INSPIRE].

[31] CMS collaboration, *Measurement of the $Y(1S), Y(2S)$ and $Y(3S)$ polarizations in pp collisions at $\sqrt{s} = 7\ TeV$*, *Phys. Rev. Lett.* **110** (2013) 081802 [arXiv:1209.2922] [INSPIRE].

[32] LHCb collaboration, *Measurement of J/ψ polarization in pp collisions at $\sqrt{s} = 7\ TeV$*, *Eur. Phys. J.* **C 73** (2013) 2631 [arXiv:1307.6379] [INSPIRE].

[33] LHCb collaboration, *Measurement of $\psi(2S)$ polarisation in pp collisions at $\sqrt{s} = 7\ TeV$*, *Eur. Phys. J.* **C 74** (2014) 2872 [arXiv:1403.1339] [INSPIRE].

[34] V.G. Kartvelishvili and S.M. Esakiya, *On hadron induced production of J/ψ meson pairs* (in Russian), *Yad. Fiz.* **38** (1983) 722 [INSPIRE].

[35] B. Humpert and P. Mery, *ψψ production at collider energies*, *Z. Phys.* **C 20** (1983) 83 [ɪɴSPIRE].

[36] B. Humpert and P. Mery, *ψψ production by quarks, gluons and B mesons*, *Phys. Lett.* **B 124** (1983) 265 [ɪɴSPIRE].

[37] P. Ko, C. Yu and J. Lee, *Inclusive double-quarkonium production at the Large Hadron Collider*, *JHEP* **01** (2011) 070 [arXiv:1007.3095] [ɪɴSPIRE].

[38] S.P. Baranov and A.H. Rezaeian, *Prompt double J/ψ production in proton-proton collisions at the LHC*, *Phys. Rev.* **D 93** (2016) 114011 [arXiv:1511.04089] [ɪɴSPIRE].

[39] L.-P. Sun, H. Han and K.-T. Chao, *Impact of J/ψ pair production at the LHC and predictions in nonrelativistic QCD*, *Phys. Rev.* **D 94** (2016) 074033 [arXiv:1404.4042] [ɪɴSPIRE].

[40] Axial Field Spectrometer collaboration, T. Akesson et al., *Double parton scattering in pp collisions at $\sqrt{s} = 63\,GeV$*, *Z. Phys.* **C 34** (1987) 163 [ɪɴSPIRE].

[41] UA2 collaboration, J. Alitti et al., *A study of multi-jet events at the CERN $\bar{p}p$ collider and a search for double parton scattering*, *Phys. Lett.* **B 268** (1991) 145 [ɪɴSPIRE].

[42] CDF collaboration, F. Abe et al., *Study of four jet events and evidence for double parton interactions in $p\bar{p}$ collisions at $\sqrt{s} = 1.8\,TeV$*, *Phys. Rev.* **D 47** (1993) 4857 [ɪɴSPIRE].

[43] ATLAS collaboration, *Study of hard double-parton scattering in four-jet events in pp collisions at $\sqrt{s} = 7\,TeV$ with the ATLAS experiment*, *JHEP* **11** (2016) 110 [arXiv:1608.01857] [ɪɴSPIRE].

[44] CDF collaboration, F. Abe et al., *Measurement of double parton scattering in $\bar{p}p$ collisions at $\sqrt{s} = 1.8\,TeV$*, *Phys. Rev. Lett.* **79** (1997) 584 [ɪɴSPIRE].

[45] D0 collaboration, V.M. Abazov et al., *Double parton interactions in γ+3 jet events in pp⁻ bar collisions $\sqrt{s} = 1.96\,TeV$.*, *Phys. Rev.* **D 81** (2010) 052012 [arXiv:0912.5104] [ɪɴSPIRE].

[46] D0 collaboration, V.M. Abazov et al., *Double parton interactions in $\gamma + 3$ jet and $\gamma + b/cjet + 2$ jet events in $p\bar{p}$ collisions at $\sqrt{s} = 1.96$ TeV*, *Phys. Rev.* **D 89** (2014) 072006 [arXiv:1402.1550] [ɪɴSPIRE].

[47] D0 collaboration, V.M. Abazov et al., *Study of double parton interactions in diphoton + dijet events in $p\bar{p}$ collisions at $\sqrt{s} = 1.96\,TeV$*, *Phys. Rev.* **D 93** (2016) 052008 [arXiv:1512.05291] [ɪɴSPIRE].

[48] CMS collaboration, *Study of double parton scattering using W + 2-jet events in proton-proton collisions at $\sqrt{s} = 7\,TeV$*, *JHEP* **03** (2014) 032 [arXiv:1312.5729] [ɪɴSPIRE].

[49] CMS collaboration, *Observation of Υ(1S) pair production in proton-proton collisions at $\sqrt{s} = 8$ TeV*, *JHEP* **05** (2017) 013 [arXiv:1610.07095] [ɪɴSPIRE].

[50] ATLAS collaboration, *Measurement of the production of a W boson in association with a charm quark in pp collisions at $\sqrt{s} = 7\,TeV$ with the ATLAS detector*, *JHEP* **05** (2014) 068 [arXiv:1402.6263] [ɪɴSPIRE].

[51] ATLAS collaboration, *Observation and measurements of the production of prompt and non-prompt J/ψ mesons in association with a Z boson in pp collisions at $\sqrt{s} = 8\,TeV$ with the ATLAS detector*, *Eur. Phys. J.* **C 75** (2015) 229 [arXiv:1412.6428] [ɪɴSPIRE].

[52] LHCb collaboration, *Observation of double charm production involving open charm in pp collisions at $\sqrt{s} = 7$ TeV*, *JHEP* **06** (2012) 141 [arXiv:1205.0975] [ɪɴSPIRE].

[53] LHCb collaboration, *Observation of associated production of a Z boson with a D meson in the forward region*, *JHEP* **04** (2014) 091 [arXiv:1401.3245] [INSPIRE].

[54] LHCb collaboration, *Production of associated Υ and open charm hadrons in pp collisions at $\sqrt{s} = 7$ and 8 TeV via double parton scattering*, *JHEP* **07** (2016) 052 [arXiv:1510.05949] [INSPIRE].

[55] NA3 collaboration, J. Badier et al., *Evidence for ψψ production in π^- interactions at 150 GeV/c and 280 GeV/c*, *Phys. Lett.* **B 114** (1982) 457 [INSPIRE].

[56] NA3 collaboration, J. Badier et al., *ψψ production and limits on beauty meson production from 400-GeV/c protons*, *Phys. Lett.* **B 158** (1985) 85 [INSPIRE].

[57] LHCb collaboration, *Observation of J/ψ pair production in pp collisions at $\sqrt{s} = 7$ TeV*, *Phys. Lett.* **B 707** (2012) 52 [arXiv:1109.0963] [INSPIRE].

[58] CMS collaboration, *Measurement of prompt J/ψ pair production in pp collisions at $\sqrt{s} = 7$ TeV*, *JHEP* **09** (2014) 094 [arXiv:1406.0484] [INSPIRE].

[59] ATLAS collaboration, *Measurement of the prompt J/ψ pair production cross-section in pp collisions at $\sqrt{s} = 8$ TeV with the ATLAS detector*, *Eur. Phys. J.* **C 77** (2017) 76 [arXiv:1612.02950] [INSPIRE].

[60] D0 collaboration, V.M. Abazov et al., *Observation and studies of double J/ψ production at the Tevatron*, *Phys. Rev.* **D 90** (2014) 111101 [arXiv:1406.2380] [INSPIRE].

[61] G. Calucci and D. Treleani, *Minijets and the two-body parton correlation*, *Phys. Rev.* **D 57** (1998) 503 [hep-ph/9707389] [INSPIRE].

[62] G. Calucci and D. Treleani, *Proton structure in transverse space and the effective cross-section*, *Phys. Rev.* **D 60** (1999) 054023 [hep-ph/9902479] [INSPIRE].

[63] A. Del Fabbro and D. Treleani, *Scale factor in double parton collisions and parton densities in transverse space*, *Phys. Rev.* **D 63** (2001) 057901 [hep-ph/0005273] [INSPIRE].

[64] S. Bansal et al., *Progress in double parton scattering studies*, arXiv:1410.6664 [INSPIRE].

[65] S.P. Baranov, A.M. Snigirev and N.P. Zotov, *Double heavy meson production through double parton scattering in hadronic collisions*, *Phys. Lett.* **B 705** (2011) 116 [arXiv:1105.6276] [INSPIRE].

[66] S.P. Baranov, A.M. Snigirev, N.P. Zotov, A. Szczurek and W. Schäfer, *Interparticle correlations in the production of J/ψ pairs in proton-proton collisions*, *Phys. Rev.* **D 87** (2013) 034035 [arXiv:1210.1806] [INSPIRE].

[67] C.-F. Qiao, L.-P. Sun and P. Sun, *Testing charmonium production mechamism via polarized J/ψ pair production at the LHC*, *J. Phys.* **G 37** (2010) 075019 [arXiv:0903.0954] [INSPIRE].

[68] A.V. Berezhnoy, A.K. Likhoded, A.V. Luchinsky and A.A. Novoselov, *Double J/ψ-meson production at LHC and 4c-tetraquark state*, *Phys. Rev.* **D 84** (2011) 094023 [arXiv:1101.5881] [INSPIRE].

[69] LHCb collaboration, *Measurement of J/ψ production in pp collisions at $\sqrt{s} = 7$ TeV*, *Eur. Phys. J.* **C 71** (2011) 1645 [arXiv:1103.0423] [INSPIRE].

[70] J.-P. Lansberg and H.-S. Shao, *J/ψ-pair production at large momenta: Indications for double parton scatterings and large α_s^5 contributions*, *Phys. Lett.* **B 751** (2015) 479 [arXiv:1410.8822] [INSPIRE].

[71] D0 collaboration, V.M. Abazov et al., *Evidence for simultaneous production of J/ψ and Υ mesons*, *Phys. Rev. Lett.* **116** (2016) 082002 [arXiv:1511.02428] [INSPIRE].

[72] LHCb collaboration, *The LHCb detector at the LHC*, 2008 *JINST* **3** S08005 [INSPIRE].

[73] LHCb collaboration, *LHCb detector performance*, *Int. J. Mod. Phys.* **A 30** (2015) 1530022 [arXiv:1412.6352] [INSPIRE].

[74] R. Aaij et al., *The LHCb trigger and its performance in 2011*, 2013 *JINST* **8** P04022 [arXiv:1211.3055] [INSPIRE].

[75] PARTICLE DATA GROUP collaboration, C. Patrignani et al., *Review of particle physics*, *Chin. Phys.* **C 40** (2016) 100001 [INSPIRE].

[76] T. Sjöstrand, S. Mrenna and P.Z. Skands, *A brief introduction to PYTHIA 8.1*, *Comput. Phys. Commun.* **178** (2008) 852 [arXiv:0710.3820] [INSPIRE].

[77] T. Sjöstrand, S. Mrenna and P.Z. Skands, *PYTHIA 6.4 physics and manual*, *JHEP* **05** (2006) 026 [hep-ph/0603175] [INSPIRE].

[78] LHCb collaboration, *Handling of the generation of primary events in Gauss, the LHCb simulation framework*, *J. Phys. Conf. Ser.* **331** (2011) 032047 [INSPIRE].

[79] D.J. Lange, *The EvtGen particle decay simulation package*, *Nucl. Instrum. Meth.* **A 462** (2001) 152 [INSPIRE].

[80] P. Golonka and Z. Was, *PHOTOS Monte Carlo: a precision tool for QED corrections in Z and W decays*, *Eur. Phys. J.* **C 45** (2006) 97 [hep-ph/0506026] [INSPIRE].

[81] GEANT4 collaboration, J. Allison et al., *Geant4 developments and applications*, *IEEE Trans. Nucl. Sci.* **53** (2006) 270.

[82] LHCb collaboration, *The LHCb simulation application, Gauss: design, evolution and experience*, *J. Phys. Conf. Ser.* **331** (2011) 032023 [INSPIRE].

[83] LHCb collaboration, *Precision luminosity measurements at LHCb*, 2014 *JINST* **9** P12005 [arXiv:1410.0149] [INSPIRE].

[84] T. Skwarnicki, *A study of the radiative cascade transitions between the Υ′ and Υ resonances*, Ph.D. Thesis, Institute of Nuclear Physics, Kraków, 1986, DESY-F31-86-02.

[85] LHCb collaboration, *Measurement of forward J/ψ production cross-sections in pp collisions at √s = 13 TeV*, *JHEP* **10** (2015) 172 [*Erratum ibid.* **1705** (2017) 063] [arXiv:1509.00771] [INSPIRE].

[86] D. Martínez Santos and F. Dupertuis, *Mass distributions marginalized over per-event errors*, *Nucl. Instrum. Meth.* **A 764** (2014) 150 [arXiv:1312.5000] [INSPIRE].

[87] K.S. Cranmer, *Kernel estimation in high-energy physics*, *Comput. Phys. Commun.* **136** (2001) 198 [hep-ex/0011057] [INSPIRE].

[88] M. Pivk and F.R. Le Diberder, *SPlot: A statistical tool to unfold data distributions*, *Nucl. Instrum. Meth.* **A 555** (2005) 356 [physics/0402083] [INSPIRE].

[89] LHCb collaboration, *Measurement of the track reconstruction efficiency at LHCb*, 2015 *JINST* **10** P02007 [arXiv:1408.1251] [INSPIRE].

[90] F. Archilli et al., *Performance of the muon identification at LHCb*, 2013 *JINST* **8** P10020 [arXiv:1306.0249] [INSPIRE].

[91] CDF collaboration, F. Abe et al., *Double parton scattering in p̄p collisions at √s = 1.8 TeV*, *Phys. Rev.* **D 56** (1997) 3811 [INSPIRE].

[92] A.K. Likhoded, A.V. Luchinsky and S.V. Poslavsky, *Production of $J/\psi + \chi_c$ and $J/\psi + J/\psi$ with real gluon emission at LHC*, *Phys. Rev.* **D 94** (2016) 054017 [arXiv:1606.06767] [inSPIRE].

[93] J.-P. Lansberg and H.-S. Shao, *Production of $J/\psi + \eta_c$ versus $J/\psi + J/\psi$ at the LHC: importance of real α_s^5 corrections*, *Phys. Rev. Lett.* **111** (2013) 122001 [arXiv:1308.0474] [inSPIRE].

[94] J.-P. Lansberg and H.-S. Shao, *Double-quarkonium production at a fixed-target experiment at the LHC (AFTER@LHC)*, *Nucl. Phys.* **B 900** (2015) 273 [arXiv:1504.06531] [inSPIRE].

[95] H.-S. Shao, *HELAC-Onia: an automatic matrix element generator for heavy quarkonium physics*, *Comput. Phys. Commun.* **184** (2013) 2562 [arXiv:1212.5293] [inSPIRE].

[96] H.-S. Shao, *HELAC-Onia 2.0: an upgraded matrix-element and event generator for heavy quarkonium physics*, *Comput. Phys. Commun.* **198** (2016) 238 [arXiv:1507.03435] [inSPIRE].

[97] L.V. Gribov, E.M. Levin and M.G. Ryskin, *Semihard processes in QCD*, *Phys. Rept.* **100** (1983) 1 [inSPIRE].

[98] E.M. Levin and M.G. Ryskin, *High-energy hadron collisions in QCD*, *Phys. Rept.* **189** (1990) 267 [inSPIRE].

[99] SMALL-X collaboration, B. Andersson et al., *Small-x phenomenology: summary and status*, *Eur. Phys. J.* **C 25** (2002) 77 [hep-ph/0204115] [inSPIRE].

[100] SMALL-X collaboration, J.R. Andersen et al., *Small-x phenomenology: Summary and status*, *Eur. Phys. J.* **C 35** (2004) 67 [hep-ph/0312333] [inSPIRE].

[101] SMALL-X collaboration, J.R. Andersen et al., *Small-x phenomenology: summary of the 3rd Lund Small-x Workshop in 2004*, *Eur. Phys. J.* **C 48** (2006) 53 [hep-ph/0604189] [inSPIRE].

[102] S.P. Baranov, *Pair production of J/ψ mesons in the k_t-factorization approach*, *Phys. Rev.* **D 84** (2011) 054012 [inSPIRE].

[103] S.P. Baranov and H. Jung, *Double J/ψ production: a probe of gluon polarization?*, *Z. Phys.* **C 66** (1995) 647 [inSPIRE].

[104] H. Jung, *Un-integrated PDFs in CCFM*, hep-ph/0411287 [inSPIRE].

[105] H. Jung et al., *The CCFM Monte Carlo generator CASCADE version 2.2.03*, *Eur. Phys. J.* **C 70** (2010) 1237 [arXiv:1008.0152] [inSPIRE].

[106] H. Jung and F. Hautmann, *Determination of transverse momentum dependent gluon density from HERA structure function measurements*, DESY-PROC-2012-02.

[107] F. Hautmann and H. Jung, *Transverse momentum dependent gluon density from DIS precision data*, *Nucl. Phys.* **B 883** (2014) 1 [arXiv:1312.7875] [inSPIRE].

[108] H. Jung and F. Hautmann, *Transverse momentum dependent gluon density from DIS precision data*, PoS(DIS2014)042.

[109] S. Dulat et al., *New parton distribution functions from a global analysis of quantum chromodynamics*, *Phys. Rev.* **D 93** (2016) 033006 [arXiv:1506.07443] [inSPIRE].

[110] NNPDF collaboration, R.D. Ball et al., *Parton distributions for the LHC Run II*, *JHEP* **04** (2015) 040 [arXiv:1410.8849] [inSPIRE].

[111] CTEQ collaboration, H.L. Lai et al., *Global QCD analysis of parton structure of the nucleon: CTEQ5 parton distributions*, *Eur. Phys. J.* **C 12** (2000) 375 [hep-ph/9903282] [INSPIRE].

[112] J. Pumplin, D.R. Stump, J. Huston, H.L. Lai, P.M. Nadolsky and W.K. Tung, *New generation of parton distributions with uncertainties from global QCD analysis*, *JHEP* **07** (2002) 012 [hep-ph/0201195] [INSPIRE].

[113] M. Butenschoen and B.A. Kniehl, *World data of J/ψ production consolidate NRQCD factorization at NLO*, *Phys. Rev.* **D 84** (2011) 051501 [arXiv:1105.0820] [INSPIRE].

[114] R. Sharma and I. Vitev, *High transverse momentum quarkonium production and dissociation in heavy ion collisions*, *Phys. Rev.* **C 87** (2013) 044905 [arXiv:1203.0329] [INSPIRE].

[115] P. Sun, C.P. Yuan and F. Yuan, *Heavy quarkonium production at low Pt in NRQCD with soft gluon resummation*, *Phys. Rev.* **D 88** (2013) 054008 [arXiv:1210.3432] [INSPIRE].

[116] G.T. Bodwin, H.S. Chung, U.-R. Kim and J. Lee, *Fragmentation contributions to J/ψ production at the Tevatron and the LHC*, *Phys. Rev. Lett.* **113** (2014) 022001 [arXiv:1403.3612] [INSPIRE].

[117] H.S. Shao, H. Han, Y.Q. Ma, C. Meng, Y.J. Zhang and K.T. Chao, *Yields and polarizations of prompt J/ψ and ψ(2S) production in hadronic collisions*, *JHEP* **05** (2015) 103 [arXiv:1411.3300] [INSPIRE].

[118] M. Krämer, 1, *Quarkonium production at high-energy colliders*, *Prog. Part. Nucl. Phys.* **47** (2001) 141 [hep-ph/0106120] [INSPIRE].

[119] E. Braaten, B.A. Kniehl and J. Lee, *Polarization of prompt J/ψ at the Tevatron*, *Phys. Rev.* **D 62** (2000) 094005 [hep-ph/9911436] [INSPIRE].

[120] P.M. Nadolsky et al., *Implications of CTEQ global analysis for collider observables*, *Phys. Rev.* **D 78** (2008) 013004 [arXiv:0802.0007] [INSPIRE].

The LHCb collaboration

R. Aaij[40], B. Adeva[39], M. Adinolfi[48], Z. Ajaltouni[5], S. Akar[59], J. Albrecht[10], F. Alessio[40],
M. Alexander[53], S. Ali[43], G. Alkhazov[31], P. Alvarez Cartelle[55], A.A. Alves Jr[59], S. Amato[2],
S. Amerio[23], Y. Amhis[7], L. An[3], L. Anderlini[18], G. Andreassi[41], M. Andreotti[17,g],
J.E. Andrews[60], R.B. Appleby[56], F. Archilli[43], P. d'Argent[12], J. Arnau Romeu[6], A. Artamonov[37],
M. Artuso[61], E. Aslanides[6], G. Auriemma[26], M. Baalouch[5], I. Babuschkin[56], S. Bachmann[12],
J.J. Back[50], A. Badalov[38], C. Baesso[62], S. Baker[55], V. Balagura[7,c], W. Baldini[17], R.J. Barlow[56],
C. Barschel[40], S. Barsuk[7], W. Barter[56], F. Baryshnikov[32], M. Baszczyk[27], V. Batozskaya[29],
B. Batsukh[61], V. Battista[41], A. Bay[41], L. Beaucourt[4], J. Beddow[53], F. Bedeschi[24], I. Bediaga[1],
L.J. Bel[43], V. Bellee[41], N. Belloli[21,i], K. Belous[37], I. Belyaev[32], E. Ben-Haim[8], G. Bencivenni[19],
S. Benson[43], A. Berezhnoy[33], R. Bernet[42], A. Bertolin[23], C. Betancourt[42], F. Betti[15],
M.-O. Bettler[40], M. van Beuzekom[43], Ia. Bezshyiko[42], S. Bifani[47], P. Billoir[8], T. Bird[56],
A. Birnkraut[10], A. Bitadze[56], A. Bizzeti[18,u], T. Blake[50], F. Blanc[41], J. Blouw[11,†], S. Blusk[61],
V. Bocci[26], T. Boettcher[58], A. Bondar[36,w], N. Bondar[31,40], W. Bonivento[16], I. Bordyuzhin[32],
A. Borgheresi[21,i], S. Borghi[56], M. Borisyak[35], M. Borsato[39], F. Bossu[7], M. Boubdir[9],
T.J.V. Bowcock[54], E. Bowen[42], C. Bozzi[17,40], S. Braun[12], M. Britsch[12], T. Britton[61],
J. Brodzicka[56], E. Buchanan[48], C. Burr[56], A. Bursche[2], J. Buytaert[40], S. Cadeddu[16],
R. Calabrese[17,g], M. Calvi[21,i], M. Calvo Gomez[38,m], A. Camboni[38], P. Campana[19],
D.H. Campora Perez[40], L. Capriotti[56], L. Carbone[15,e], G. Carboni[25,j], R. Cardinale[20,h],
A. Cardini[16], P. Carniti[21,i], L. Carson[52], K. Carvalho Akiba[2], G. Casse[54], L. Cassina[21,i],
L. Castillo Garcia[41], M. Cattaneo[40], G. Cavallero[20], R. Cenci[24,t], D. Chamont[7], M. Charles[8],
Ph. Charpentier[40], G. Chatzikonstantinidis[47], M. Chefdeville[4], S. Chen[56], S.-F. Cheung[57],
V. Chobanova[39], M. Chrzaszcz[42,27], X. Cid Vidal[39], G. Ciezarek[43], P.E.L. Clarke[52],
M. Clemencic[40], H.V. Cliff[49], J. Closier[40], V. Coco[59], J. Cogan[6], E. Cogneras[5], V. Cogoni[16,40,f],
L. Cojocariu[30], G. Collazuol[23,o], P. Collins[40], A. Comerma-Montells[12], A. Contu[40], A. Cook[48],
G. Coombs[40], S. Coquereau[38], G. Corti[40], M. Corvo[17,g], C.M. Costa Sobral[50], B. Couturier[40],
G.A. Cowan[52], D.C. Craik[52], A. Crocombe[50], M. Cruz Torres[62], S. Cunliffe[55], R. Currie[55],
C. D'Ambrosio[40], F. Da Cunha Marinho[2], E. Dall'Occo[43], J. Dalseno[48], P.N.Y. David[43],
A. Davis[3], K. De Bruyn[6], S. De Capua[56], M. De Cian[12], J.M. De Miranda[1], L. De Paula[2],
M. De Serio[14,d], P. De Simone[19], C.-T. Dean[53], D. Decamp[4], M. Deckenhoff[10], L. Del Buono[8],
M. Demmer[10], A. Dendek[28], D. Derkach[35], O. Deschamps[5], F. Dettori[40], B. Dey[22], A. Di Canto[40],
H. Dijkstra[40], F. Dordei[40], M. Dorigo[41], A. Dosil Suárez[39], A. Dovbnya[45], K. Dreimanis[54],
L. Dufour[43], G. Dujany[56], K. Dungs[40], P. Durante[40], R. Dzhelyadin[37], A. Dziurda[40],
A. Dzyuba[31], N. Déléage[4], S. Easo[51], M. Ebert[52], U. Egede[55], V. Egorychev[32], S. Eidelman[36,w],
S. Eisenhardt[52], U. Eitschberger[10], R. Ekelhof[10], L. Eklund[53], S. Ely[61], S. Esen[12], H.M. Evans[49],
T. Evans[57], A. Falabella[15], N. Farley[47], S. Farry[54], R. Fay[54], D. Fazzini[21,i], D. Ferguson[52],
A. Fernandez Prieto[39], F. Ferrari[15,40], F. Ferreira Rodrigues[2], M. Ferro-Luzzi[40], S. Filippov[34],
R.A. Fini[14], M. Fiore[17,g], M. Fiorini[17,g], M. Firlej[28], C. Fitzpatrick[41], T. Fiutowski[28],
F. Fleuret[7,b], K. Fohl[40], M. Fontana[16,40], F. Fontanelli[20,h], D.C. Forshaw[61], R. Forty[40],
V. Franco Lima[54], M. Frank[40], C. Frei[40], J. Fu[22,q], W. Funk[40], E. Furfaro[25,j], C. Färber[40],
A. Gallas Torreira[39], D. Galli[15,e], S. Gallorini[23], S. Gambetta[52], M. Gandelman[2], P. Gandini[57],
Y. Gao[3], L.M. Garcia Martin[69], J. García Pardiñas[39], J. Garra Tico[49], L. Garrido[38],
P.J. Garsed[49], D. Gascon[38], C. Gaspar[40], L. Gavardi[10], G. Gazzoni[5], D. Gerick[12], E. Gersabeck[12],
M. Gersabeck[56], T. Gershon[50], Ph. Ghez[4], S. Gianì[41], V. Gibson[49], O.G. Girard[41], L. Giubega[30],
K. Gizdov[52], V.V. Gligorov[8], D. Golubkov[32], A. Golutvin[55,40], A. Gomes[1,a], I.V. Gorelov[33],
C. Gotti[21,i], R. Graciani Diaz[38], L.A. Granado Cardoso[40], E. Graugés[38], E. Graverini[42],
G. Graziani[18], A. Grecu[30], P. Griffith[47], L. Grillo[21,40,i], B.R. Gruberg Cazon[57], O. Grünberg[67],

E. Gushchin[34], Yu. Guz[37], T. Gys[40], C. Göbel[62], T. Hadavizadeh[57], C. Hadjivasiliou[5],
G. Haefeli[41], C. Haen[40], S.C. Haines[49], B. Hamilton[60], X. Han[12], S. Hansmann-Menzemer[12],
N. Harnew[57], S.T. Harnew[48], J. Harrison[56], M. Hatch[40], J. He[63], T. Head[41], A. Heister[9],
K. Hennessy[54], P. Henrard[5], L. Henry[8], E. van Herwijnen[40], M. Heß[67], A. Hicheur[2], D. Hill[57],
C. Hombach[56], H. Hopchev[41], W. Hulsbergen[43], T. Humair[55], M. Hushchyn[35], D. Hutchcroft[54],
M. Idzik[28], P. Ilten[58], R. Jacobsson[40], A. Jaeger[12], J. Jalocha[57], E. Jans[43], A. Jawahery[60],
F. Jiang[3], M. John[57], D. Johnson[40], C.R. Jones[49], C. Joram[40], B. Jost[40], N. Jurik[57],
S. Kandybei[45], M. Karacson[40], J.M. Kariuki[48], S. Karodia[53], M. Kecke[12], M. Kelsey[61],
M. Kenzie[49], T. Ketel[44], E. Khairullin[35], B. Khanji[12], C. Khurewathanakul[41], T. Kirn[9],
S. Klaver[56], K. Klimaszewski[29], S. Koliiev[46], M. Kolpin[12], I. Komarov[41], R.F. Koopman[44],
P. Koppenburg[43], A. Kosmyntseva[32], A. Kozachuk[33], M. Kozeiha[5], L. Kravchuk[34], K. Kreplin[12],
M. Kreps[50], P. Krokovny[36,w], F. Kruse[10], W. Krzemien[29], W. Kucewicz[27,l], M. Kucharczyk[27],
V. Kudryavtsev[36,w], A.K. Kuonen[41], K. Kurek[29], T. Kvaratskheliya[32,40], D. Lacarrere[40],
G. Lafferty[56], A. Lai[16], G. Lanfranchi[19], C. Langenbruch[9], T. Latham[50], C. Lazzeroni[47],
R. Le Gac[6], J. van Leerdam[43], A. Leflat[33,40], J. Lefrançois[7], R. Lefèvre[5], F. Lemaitre[40],
E. Lemos Cid[39], O. Leroy[6], T. Lesiak[27], B. Leverington[12], T. Li[3], Y. Li[7], T. Likhomanenko[35,68],
R. Lindner[40], C. Linn[40], F. Lionetto[42], X. Liu[3], D. Loh[50], I. Longstaff[53], J.H. Lopes[2],
D. Lucchesi[23,o], M. Lucio Martinez[39], H. Luo[52], A. Lupato[23], E. Luppi[17,g], O. Lupton[40],
A. Lusiani[24], X. Lyu[63], F. Machefert[7], F. Maciuc[30], O. Maev[31], K. Maguire[56], S. Malde[57],
A. Malinin[68], T. Maltsev[36], G. Manca[16,f], G. Mancinelli[6], P. Manning[61], J. Maratas[5,v],
J.F. Marchand[4], U. Marconi[15], C. Marin Benito[38], M. Marinangeli[41], P. Marino[24,t], J. Marks[12],
G. Martellotti[26], M. Martin[6], M. Martinelli[41], D. Martinez Santos[39], F. Martinez Vidal[69],
D. Martins Tostes[2], L.M. Massacrier[7], A. Massafferri[1], R. Matev[40], A. Mathad[50], Z. Mathe[40],
C. Matteuzzi[21], A. Mauri[42], E. Maurice[7,b], B. Maurin[41], A. Mazurov[47], M. McCann[55,40],
A. McNab[56], R. McNulty[13], B. Meadows[59], F. Meier[10], M. Meissner[12], D. Melnychuk[29],
M. Merk[43], A. Merli[22,q], E. Michielin[23], D.A. Milanes[66], M.-N. Minard[4], D.S. Mitzel[12],
A. Mogini[8], J. Molina Rodriguez[1], I.A. Monroy[66], S. Monteil[5], M. Morandin[23], P. Morawski[28],
A. Mordà[6], M.J. Morello[24,t], O. Morgunova[68], J. Moron[28], A.B. Morris[52], R. Mountain[61],
F. Muheim[52], M. Mulder[43], M. Mussini[15], D. Müller[56], J. Müller[10], K. Müller[42], V. Müller[10],
P. Naik[48], T. Nakada[41], R. Nandakumar[51], A. Nandi[57], I. Nasteva[2], M. Needham[52], N. Neri[22],
S. Neubert[12], N. Neufeld[40], M. Neuner[12], T.D. Nguyen[41], C. Nguyen-Mau[41,n], S. Nieswand[9],
R. Niet[10], N. Nikitin[33], T. Nikodem[12], A. Nogay[68], A. Novoselov[37], D.P. O'Hanlon[50],
A. Oblakowska-Mucha[28], V. Obraztsov[37], S. Ogilvy[19], R. Oldeman[16,f], C.J.G. Onderwater[70],
J.M. Otalora Goicochea[2], A. Otto[40], P. Owen[42], A. Oyanguren[69], P.R. Pais[41], A. Palano[14,d],
M. Palutan[19], A. Papanestis[51], M. Pappagallo[14,d], L.L. Pappalardo[17,g], W. Parker[60], C. Parkes[56],
G. Passaleva[18], A. Pastore[14,d], G.D. Patel[54], M. Patel[55], C. Patrignani[15,e], A. Pearce[40],
A. Pellegrino[43], G. Penso[26], M. Pepe Altarelli[40], S. Perazzini[40], P. Perret[5], L. Pescatore[47],
K. Petridis[48], A. Petrolini[20,h], A. Petrov[68], M. Petruzzo[22,q], E. Picatoste Olloqui[38], B. Pietrzyk[4],
M. Pikies[27], D. Pinci[26], A. Pistone[20], A. Piucci[12], V. Placinta[30], S. Playfer[52], M. Plo Casasus[39],
T. Poikela[40], F. Polci[8], A. Poluektov[50,36], I. Polyakov[61], E. Polycarpo[2], G.J. Pomery[48],
A. Popov[37], D. Popov[11,40], B. Popovici[30], S. Poslavskii[37], C. Potterat[2], E. Price[48], J.D. Price[54],
J. Prisciandaro[39,40], A. Pritchard[54], C. Prouve[48], V. Pugatch[46], A. Puig Navarro[42], G. Punzi[24,p],
W. Qian[50], R. Quagliani[7,48], B. Rachwal[27], J.H. Rademacker[48], M. Rama[24], M. Ramos Pernas[39],
M.S. Rangel[2], I. Raniuk[45], F. Ratnikov[35], G. Raven[44], F. Redi[55], S. Reichert[10], A.C. dos Reis[1],
C. Remon Alepuz[69], V. Renaudin[7], S. Ricciardi[51], S. Richards[48], M. Rihl[40], K. Rinnert[54],
V. Rives Molina[38], P. Robbe[7,40], A.B. Rodrigues[1], E. Rodrigues[59], J.A. Rodriguez Lopez[66],
P. Rodriguez Perez[56,†], A. Rogozhnikov[35], S. Roiser[40], A. Rollings[57], V. Romanovskiy[37],
A. Romero Vidal[39], J.W. Ronayne[13], M. Rotondo[19], M.S. Rudolph[61], T. Ruf[40], P. Ruiz Valls[69],

J.J. Saborido Silva[39], E. Sadykhov[32], N. Sagidova[31], B. Saitta[16,f], V. Salustino Guimaraes[1],
C. Sanchez Mayordomo[69], B. Sanmartin Sedes[39], R. Santacesaria[26], C. Santamarina Rios[39],
M. Santimaria[19], E. Santovetti[25,j], A. Sarti[19,k], C. Satriano[26,s], A. Satta[25], D.M. Saunders[48],
D. Savrina[32,33], S. Schael[9], M. Schellenberg[10], M. Schiller[53], H. Schindler[40], M. Schlupp[10],
M. Schmelling[11], T. Schmelzer[10], B. Schmidt[40], O. Schneider[41], A. Schopper[40], K. Schubert[10],
M. Schubiger[41], M.-H. Schune[7], R. Schwemmer[40], B. Sciascia[19], A. Sciubba[26,k], A. Semennikov[32],
A. Sergi[47], N. Serra[42], J. Serrano[6], L. Sestini[23], P. Seyfert[21], M. Shapkin[37], I. Shapoval[45],
Y. Shcheglov[31], T. Shears[54], L. Shekhtman[36,w], V. Shevchenko[68], B.G. Siddi[17,40],
R. Silva Coutinho[42], L. Silva de Oliveira[2], G. Simi[23,o], S. Simone[14,d], M. Sirendi[49], N. Skidmore[48],
T. Skwarnicki[61], E. Smith[55], I.T. Smith[52], J. Smith[49], M. Smith[55], H. Snoek[43], l. Soares Lavra[1],
M.D. Sokoloff[59], F.J.P. Soler[53], B. Souza De Paula[2], B. Spaan[10], P. Spradlin[53], S. Sridharan[40],
F. Stagni[40], M. Stahl[12], S. Stahl[40], P. Stefko[41], S. Stefkova[55], O. Steinkamp[42], S. Stemmle[12],
O. Stenyakin[37], H. Stevens[10], S. Stevenson[57], S. Stoica[30], S. Stone[61], B. Storaci[42], S. Stracka[24,p],
M. Straticiuc[30], U. Straumann[42], L. Sun[64], W. Sutcliffe[55], K. Swientek[28], V. Syropoulos[44],
M. Szczekowski[29], T. Szumlak[28], S. T'Jampens[4], A. Tayduganov[6], T. Tekampe[10], G. Tellarini[17,g],
F. Teubert[40], E. Thomas[40], J. van Tilburg[43], M.J. Tilley[55], V. Tisserand[4], M. Tobin[41], S. Tolk[49],
L. Tomassetti[17,g], D. Tonelli[40], S. Topp-Joergensen[57], F. Toriello[61], E. Tournefier[4], S. Tourneur[41],
K. Trabelsi[41], M. Traill[53], M.T. Tran[41], M. Tresch[42], A. Trisovic[40], A. Tsaregorodtsev[6],
P. Tsopelas[43], A. Tully[49], N. Tuning[43], A. Ukleja[29], A. Ustyuzhanin[35], U. Uwer[12], C. Vacca[16,f],
V. Vagnoni[15,40], A. Valassi[40], S. Valat[40], G. Valenti[15], R. Vazquez Gomez[19],
P. Vazquez Regueiro[39], S. Vecchi[17], M. van Veghel[43], J.J. Velthuis[48], M. Veltri[18,r], G. Veneziano[57],
A. Venkateswaran[61], M. Vernet[5], M. Vesterinen[12], J.V. Viana Barbosa[40], B. Viaud[7], D. Vieira[63],
M. Vieites Diaz[39], H. Viemann[67], X. Vilasis-Cardona[38,m], M. Vitti[49], V. Volkov[33], A. Vollhardt[42],
B. Voneki[40], A. Vorobyev[31], V. Vorobyev[36,w], C. Voß[9], J.A. de Vries[43], C. Vázquez Sierra[39],
R. Waldi[67], C. Wallace[50], R. Wallace[13], J. Walsh[24], J. Wang[61], D.R. Ward[49], H.M. Wark[54],
N.K. Watson[47], D. Websdale[55], A. Weiden[42], M. Whitehead[40], J. Wicht[50], G. Wilkinson[57,40],
M. Wilkinson[61], M. Williams[40], M.P. Williams[47], M. Williams[58], T. Williams[47], F.F. Wilson[51],
J. Wimberley[60], J. Wishahi[10], W. Wislicki[29], M. Witek[27], G. Wormser[7], S.A. Wotton[49],
K. Wraight[53], K. Wyllie[40], Y. Xie[65], Z. Xing[61], Z. Xu[4], Z. Yang[3], Y. Yao[61], H. Yin[65], J. Yu[65],
X. Yuan[36,w], O. Yushchenko[37], K.A. Zarebski[47], M. Zavertyaev[11,c], L. Zhang[3], Y. Zhang[7],
Y. Zhang[63], A. Zhelezov[12], Y. Zheng[63], X. Zhu[3], V. Zhukov[33], S. Zucchelli[15].

1   Centro Brasileiro de Pesquisas Físicas (CBPF), Rio de Janeiro, Brazil
2   Universidade Federal do Rio de Janeiro (UFRJ), Rio de Janeiro, Brazil
3   Center for High Energy Physics, Tsinghua University, Beijing, China
4   LAPP, Université Savoie Mont-Blanc, CNRS/IN2P3, Annecy-Le-Vieux, France
5   Clermont Université, Université Blaise Pascal, CNRS/IN2P3, LPC, Clermont-Ferrand, France
6   CPPM, Aix-Marseille Université, CNRS/IN2P3, Marseille, France
7   LAL, Université Paris-Sud, CNRS/IN2P3, Orsay, France
8   LPNHE, Université Pierre et Marie Curie, Université Paris Diderot, CNRS/IN2P3, Paris, France
9   I. Physikalisches Institut, RWTH Aachen University, Aachen, Germany
10   Fakultät Physik, Technische Universität Dortmund, Dortmund, Germany
11   Max-Planck-Institut für Kernphysik (MPIK), Heidelberg, Germany
12   Physikalisches Institut, Ruprecht-Karls-Universität Heidelberg, Heidelberg, Germany
13   School of Physics, University College Dublin, Dublin, Ireland
14   Sezione INFN di Bari, Bari, Italy
15   Sezione INFN di Bologna, Bologna, Italy
16   Sezione INFN di Cagliari, Cagliari, Italy
17   Sezione INFN di Ferrara, Ferrara, Italy
18   Sezione INFN di Firenze, Firenze, Italy

[19] *Laboratori Nazionali dell'INFN di Frascati, Frascati, Italy*

[20] *Sezione INFN di Genova, Genova, Italy*

[21] *Sezione INFN di Milano Bicocca, Milano, Italy*

[22] *Sezione INFN di Milano, Milano, Italy*

[23] *Sezione INFN di Padova, Padova, Italy*

[24] *Sezione INFN di Pisa, Pisa, Italy*

[25] *Sezione INFN di Roma Tor Vergata, Roma, Italy*

[26] *Sezione INFN di Roma La Sapienza, Roma, Italy*

[27] *Henryk Niewodniczanski Institute of Nuclear Physics Polish Academy of Sciences, Kraków, Poland*

[28] *AGH - University of Science and Technology, Faculty of Physics and Applied Computer Science, Kraków, Poland*

[29] *National Center for Nuclear Research (NCBJ), Warsaw, Poland*

[30] *Horia Hulubei National Institute of Physics and Nuclear Engineering, Bucharest-Magurele, Romania*

[31] *Petersburg Nuclear Physics Institute (PNPI), Gatchina, Russia*

[32] *Institute of Theoretical and Experimental Physics (ITEP), Moscow, Russia*

[33] *Institute of Nuclear Physics, Moscow State University (SINP MSU), Moscow, Russia*

[34] *Institute for Nuclear Research of the Russian Academy of Sciences (INR RAN), Moscow, Russia*

[35] *Yandex School of Data Analysis, Moscow, Russia*

[36] *Budker Institute of Nuclear Physics (SB RAS), Novosibirsk, Russia*

[37] *Institute for High Energy Physics (IHEP), Protvino, Russia*

[38] *ICCUB, Universitat de Barcelona, Barcelona, Spain*

[39] *Universidad de Santiago de Compostela, Santiago de Compostela, Spain*

[40] *European Organization for Nuclear Research (CERN), Geneva, Switzerland*

[41] *Institute of Physics, Ecole Polytechnique Fédérale de Lausanne (EPFL), Lausanne, Switzerland*

[42] *Physik-Institut, Universität Zürich, Zürich, Switzerland*

[43] *Nikhef National Institute for Subatomic Physics, Amsterdam, The Netherlands*

[44] *Nikhef National Institute for Subatomic Physics and VU University Amsterdam, Amsterdam, The Netherlands*

[45] *NSC Kharkiv Institute of Physics and Technology (NSC KIPT), Kharkiv, Ukraine*

[46] *Institute for Nuclear Research of the National Academy of Sciences (KINR), Kyiv, Ukraine*

[47] *University of Birmingham, Birmingham, United Kingdom*

[48] *H.H. Wills Physics Laboratory, University of Bristol, Bristol, United Kingdom*

[49] *Cavendish Laboratory, University of Cambridge, Cambridge, United Kingdom*

[50] *Department of Physics, University of Warwick, Coventry, United Kingdom*

[51] *STFC Rutherford Appleton Laboratory, Didcot, United Kingdom*

[52] *School of Physics and Astronomy, University of Edinburgh, Edinburgh, United Kingdom*

[53] *School of Physics and Astronomy, University of Glasgow, Glasgow, United Kingdom*

[54] *Oliver Lodge Laboratory, University of Liverpool, Liverpool, United Kingdom*

[55] *Imperial College London, London, United Kingdom*

[56] *School of Physics and Astronomy, University of Manchester, Manchester, United Kingdom*

[57] *Department of Physics, University of Oxford, Oxford, United Kingdom*

[58] *Massachusetts Institute of Technology, Cambridge, MA, United States*

[59] *University of Cincinnati, Cincinnati, OH, United States*

[60] *University of Maryland, College Park, MD, United States*

[61] *Syracuse University, Syracuse, NY, United States*

[62] *Pontifícia Universidade Católica do Rio de Janeiro (PUC-Rio), Rio de Janeiro, Brazil, associated to* [2]

[63] *University of Chinese Academy of Sciences, Beijing, China, associated to* [3]

[64] *School of Physics and Technology, Wuhan University, Wuhan, China, associated to* [3]

[65] *Institute of Particle Physics, Central China Normal University, Wuhan, Hubei, China, associated to* [3]

[66] *Departamento de Fisica , Universidad Nacional de Colombia, Bogota, Colombia, associated to* [8]

[67] *Institut für Physik, Universität Rostock, Rostock, Germany, associated to* [12]

[68] *National Research Centre Kurchatov Institute, Moscow, Russia, associated to* [32]

[69] *Instituto de Fisica Corpuscular (IFIC), Universitat de Valencia-CSIC, Valencia, Spain, associated to* [38]

[70] *Van Swinderen Institute, University of Groningen, Groningen, The Netherlands, associated to* [43]

[a] *Universidade Federal do Triângulo Mineiro (UFTM), Uberaba-MG, Brazil*

[b] *Laboratoire Leprince-Ringuet, Palaiseau, France*

[c] *P.N. Lebedev Physical Institute, Russian Academy of Science (LPI RAS), Moscow, Russia*

[d] *Università di Bari, Bari, Italy*

[e] *Università di Bologna, Bologna, Italy*

[f] *Università di Cagliari, Cagliari, Italy*

[g] *Università di Ferrara, Ferrara, Italy*

[h] *Università di Genova, Genova, Italy*

[i] *Università di Milano Bicocca, Milano, Italy*

[j] *Università di Roma Tor Vergata, Roma, Italy*

[k] *Università di Roma La Sapienza, Roma, Italy*

[l] *AGH - University of Science and Technology, Faculty of Computer Science, Electronics and Telecommunications, Kraków, Poland*

[m] *LIFAELS, La Salle, Universitat Ramon Llull, Barcelona, Spain*

[n] *Hanoi University of Science, Hanoi, Viet Nam*

[o] *Università di Padova, Padova, Italy*

[p] *Università di Pisa, Pisa, Italy*

[q] *Università degli Studi di Milano, Milano, Italy*

[r] *Università di Urbino, Urbino, Italy*

[s] *Università della Basilicata, Potenza, Italy*

[t] *Scuola Normale Superiore, Pisa, Italy*

[u] *Università di Modena e Reggio Emilia, Modena, Italy*

[v] *Iligan Institute of Technology (IIT), Iligan, Philippines*

[w] *Novosibirsk State University, Novosibirsk, Russia*

[†] *Deceased*